Charles University in Prague
Faculty of Mathematics and Physics

MASTER THESIS

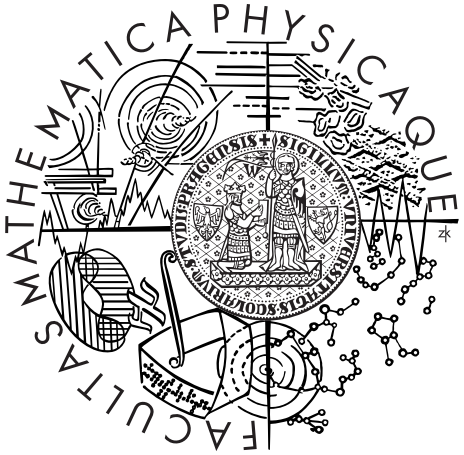

Bc. Kristina Bártová

Polarising Versions of Glossy BRDF Models

Department of Software and Computer Science Education

Supervisor of the master thesis: doc. Dr. Alexander Wilkie
Study programme: Software Systems
Specialization: Computer Graphics

Prague 2013

I would like to thank to my supervisor, Alexander Wilkie for guiding me and supporting me over the years.

I would like to thank to Thomas A. Germer, my advisor and friend, who helped me to find the right direction in this thesis by providing many valuable pieces of advice. I am very grateful to you.

I would also like to thank to Ivo Pavlík, who didn't let me down.

I would especially like to express my deepest gratitude to my family and people I love for their love, support and constant encouragement I have gotten over the years.

I declare that I carried out this master thesis independently, and only with the cited sources, literature and other professional sources.

I understand that my work relates to the rights and obligations under the Act No. 121/2000 Coll., the Copyright Act, as amended, in particular the fact that the Charles University in Prague has the right to conclude a license agreement on the use of this work as a school work pursuant to Section 60 paragraph 1 of the Copyright Act.

In ..... date ..... signature of the author

Název práce: Polarising Versions of Glossy BRDF Models

Autor: Bc. Kristina Bártová

Katedra: Kabinet software a výuky informatiky, skupina počítačové grafiky

Vedoucí diplomové práce: doc. Dr. Alexander Wilkie, KSVI

Abstrakt: Cílem počítačové grafiky je přesně modelovat vzhled skutečných objektů. K tomu je nutné modelovat interakce světla s různými materiály. Jedním z důležitých parametrů světla je také jeho polarizace. Zahrnutí polarizace do osvětlovacího modelu může výrazně přispět k realistickému vzhledu renderovaných obrazů například v situacích, kdy ve scéně dochází k mnohačetným odrazům světelných paprsků na různých zrcadlových plochách, apod. Současné renderovací systémy ale polarizaci neuvažují z důvodu velké složitosti takového řešení. Klíčovým prvkem pro získání fyzikálně věrných obrazů jsou realistické, polarizace schopné BRDF (BidirectionalReflectanceDistributionFunction) modely. V rámci této práce, byly teoreticky odvozeny polarizaci zahrnující verze následujících modelů: Torrance-Sparrow, He-Torrance-Sillion-Greenberg a Weidlich-Wilkie. Pro každý z těchto modelů byly systematicky odvozeny Muellerovy matice (matematická konstrukce používaná k popisu odrazivosti polarizujícího povrchu). Chování odvozených matic v závislosti na různých vstupních parametrech bylo následně testováno v programu Wolfram Mathematica. Odvozené BRDF modely zahrnující polarizaci byly implementovány v systému ART (Advanced Rendering Toolkit). Soudě podle dostupných zdrojů se jedná o pravděpodobně vůbec první využití zmíněných BRDF modelů, které v průběhu renderování zohledňuje polarizaci. Simulace provedené v programu Wolfram Mathematica, podobně jako výsledné vyrenderované obrázky, poukazují na správnost navrženého řešení.

Klíčová slova: fyzikalní synteza obrazu, obousměrná distribuční funkce odrazu světla, zobrazovaní polarizace

Title: Polarising Versions of Glossy BRDF Models

Author: Bc. Kristina Bártová

Department: Department of Software and Computer Science Education, Computer Graphics Group

Supervisor: doc. Dr. Alexander Wilkie, KSVI

Abstract: The goal of computer graphics is to precisely model the appearance of real objects. It includes of interactions of light with various materials. Polarisation is one of the fundamental properties of light. Incorporating polarisation parameter into an illumination model can significantly enhance the physical realism of rendered images in the case of scenes including multiple light bounces via specular surfaces, etc. However, recent rendering systems do not take polarisation into account because of complexity of such a solution. The key component for obtaining physically correct images are realistic, polarisation capable BRDF (Bidirectional Reflectance Distribution Function) models. Within this thesis, polarising versions of the following BRDF models were theoretically derived: Torrance Sparrow, He-Torrance-Sillion-Greenberg and Weidlich-Wilkie. For each of these models, Mueller matrices (the mathematical construct used to describe polarising surface reflectance) were systematically derived and their behaviour tested under various input parameters using Wolfram Mathematica. Derived polarising glossy BRDF models were further implemented using a rendering research system, ART (Advanced Rendering Toolkit). As far as we know, it is the very first usage of these BRDF models in a polarisation renderer. Simulations carried out in Wolfram Mathematica as well as rendered images support the validity of the proposed solution.

Keywords: Physically based rendering, BRDF models, polarisation rendering

Contents

Introduction

Polarisation is one of the fundamental properties of light, but despite this fact, it is not currently usually taken in account when rendering realistic computer imagery. There are two main reasons for that - first, it seems that polarisation doesn't contribute enough to the appearance of an average scene to warrant its inclusion in rendering systems, which actually holds for a large number of scenes. Nevertheless, there are some exceptions where polarisation matters and is responsible for perceptible visual effects, namely, scenes that involve multiple light bounces via highly specular surfaces, glowing specular surfaces or the atmosphere. Neglecting polarisation in such scenes leads to inaccurate results, because the light propagation might be mispredicted. The second reason is that the technology for including polarisation in industrial-strength rendering engines is not entirely ready yet.

The key component for obtaining physically correct images are realistic BRDF models. These models must describe polarising reflectance and also must be suitable for computer graphics purposes. However, there are only few BRDF models that meet both requirements and, hence, can be used for polarisation ray tracing. These are Fresnel, Torrance Sparrow and He-Torrance-Sillion-Greenberg BRDF models. Only the first two have ever been used in a polarisation renderer, while the third was theoretically derived by the authors, but never actually used in a renderer so far.

When the light, represented by a four-dimensional Stokes vector, interacts with surface medium, its polarisation state is almost always changed. In order to describe this alteration mathematically, a data construct is needed. Mueller matrix is a 4x4 transformation matrix representing the model of the medium that allows to determine changes in the intensity and polarisation state of an incident light. Hence, the main aim of polarimetry lies in the physical interpretation of the information that provides the 16 elements of the Mueller matrix. [1]

The task of this thesis is be to systematically derive Mueller matrices for each model and test them in an existing polarisation-capable rendering system. In addition to this, due to its flexibility, it would be also very useful to know a polarising form of a basic layered BRDF model, such as the Weidlich-Wilkie model.

The thesis begins with an introduction to terms and definitions related to polarisation and its mathematical representation in Chapter 1. First, basic terms, such as what polarised light is and what are its properties, are defined. After that mathematical structures used to represent polarised light are proposed.

Chapter 2 provides a brief review int he field of image rendering using polarisation. This report starts with the fundamental concepts about path tracing, polarising path tracing and BRDF, followed by the introduction of Advanced Rendering Toolkit, a predictive rendering system that was used to test the results of the theses, and SCATMECH, a library that is capable of evaluating Mueller matrix for Torrance-Sparrow model.

The Torrance-Sparrow model, and its Mueller matrix derivation is discussed in Chapter 3, the He-Torrance-Sparrow-Greenberg model in Chapter 4 and the layered Weidlich-Wilkie model in Chapter 5.

All model results that were implemented in a polarisation-capable rendering system ART are presented in Chapter 6.

At the end, a short conclusion is presented and future research tasks are discussed.

1. Physics basics

In order to provide a comprehensive introduction into the field of light polarisation and its mathematical representation, this chapter starts with a review of the basic terms and definitions. For a more details, please refer to one of the polarisation literature. [2], [3], [6]

1.1 Light

Light is an electromagnetic radiation defined by its wavelength, intensity and state of polarisation. It is commonly described as a collection of one or more photons propagating through the space as electromagnetic waves. The fact that light exhibits both particle and wave nature, explains light interaction at the macroscopic and microscopic level, respectively. The particle nature (using geometric or ray optics) accounts for shadow formation, while the wave nature of light accounts for phenomena such as light interference, diffraction or polarisation.

1.2 Polarised Light

Polarisation is a property of light that can oscillate in a transversal fashion linearly in a single plane or along a circle or an ellipse. [2] Fig. 1.1 illustrates this behaviour for a single wave-train.

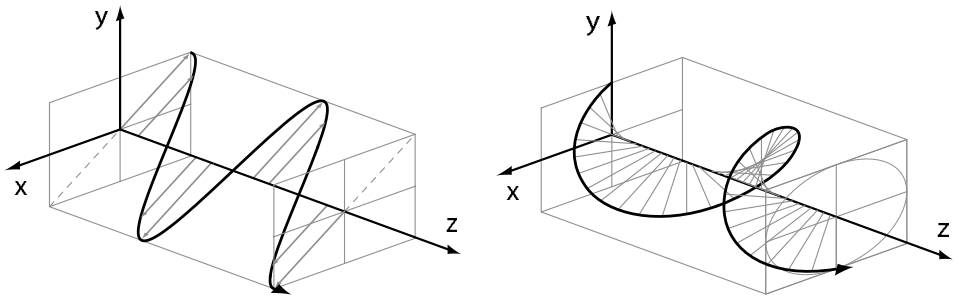

(a) Linear polarisation (b) Elliptical polarisation

Figure 1.1: (a): A linearly polarised wave-train; (b): An elliptically polarised wave-train. Both images show a single wave-train, which conceptually corresponds to the oscillations of a single photon. Image courtesy of [2].

The polarisation of light arises out of the transverse nature of the electromagnetic radiation, but it is related to the orientation of the electric field E only, thus the magnetic field B is not taken into account to denote polarisation.

1.2.1 Types of Polarisation

The standard approach to understanding the polarisation, is to decompose the electric field E into two orthogonal components that are aligned with the x and y axes, respectively.

The x and y field components will be of the form

$$E_x(t) = V_x(t) \cdot cos(2\pi \cdot \nu \cdot t + \delta_x) \tag{1.1}$$

$$E_y(t) = V_y(t) \cdot cos(2\pi \cdot \nu \cdot t + \delta_y) \tag{1.2}$$

where V_x and V_y are the amplitudes $[V \cdot m^{-1}]$, ν is the frequency $[Hz]$, δ_x and δ_y are the phases $[rad]$ of the electromagnetic wave-train, and t is the time $[s]$. The relationship between the x and y components of the electric field is illustrated on the Figure 1.2. [1] It is essential to keep in mind that equations 1.1 and 1.2 refers to the oscillations of a single photon.

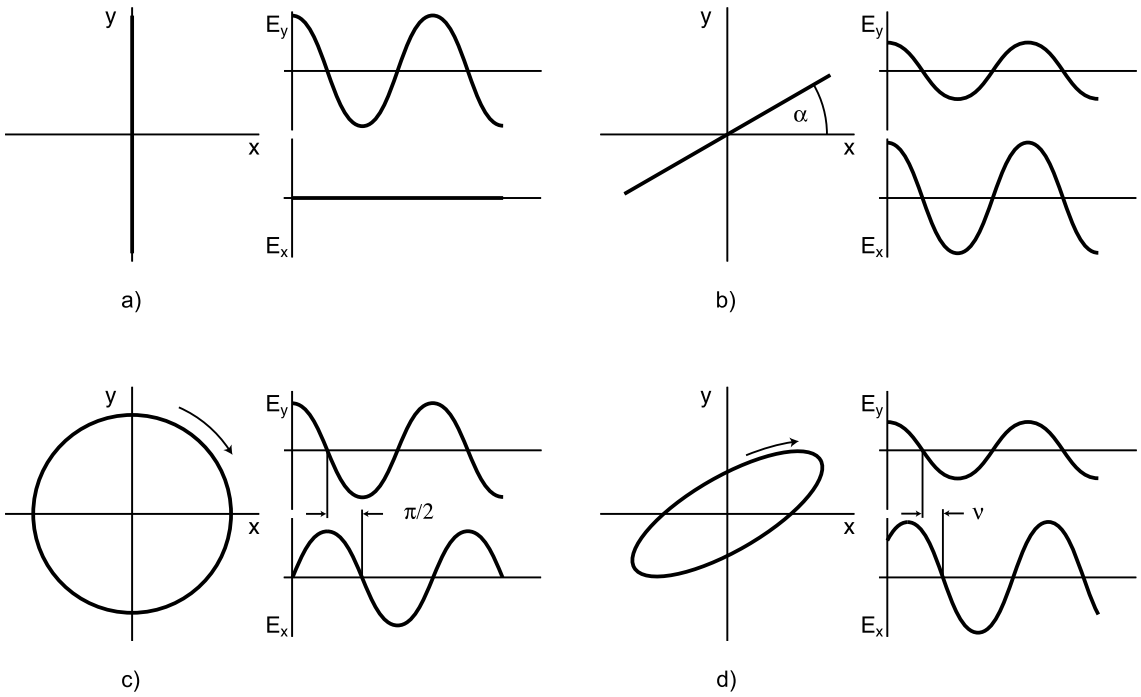

Figure 1.2: Four typical scenarios of how a single wave-train of an electromagnetic radiation can be polarised and what the x and y components look like in these cases. Image courtesy of [2].

Figure 1.2 shows that the polarisation states arise from relationship between the magnitude and phase of the orthogonal components of the electric field (i.e. E_x and E_y). It can also be seen that behaviour during the reflection and refraction of the light is independent.

A single photon is always polarised, because its oscillation will exhibit one of the patterns that is shown in figure 1.2 (or a variation thereof). Since an entire light ray is composed of a number of photons, a ray only exhibits properties of polarised light if all of the photons (or at least most of them) are polarised in the same fashion.

1.2.2 Optical Element

All light interactions with a surface cause a change of the polarisation state of light (see Fig. 1.3). Such surface is often called optical element or polarising

[1] The (x, y) components of a wave-train are usually referred to as the perpendicular ($\perp$) and parallel ($\parallel$) or the s (from the German senkrecht) and p, respectively.

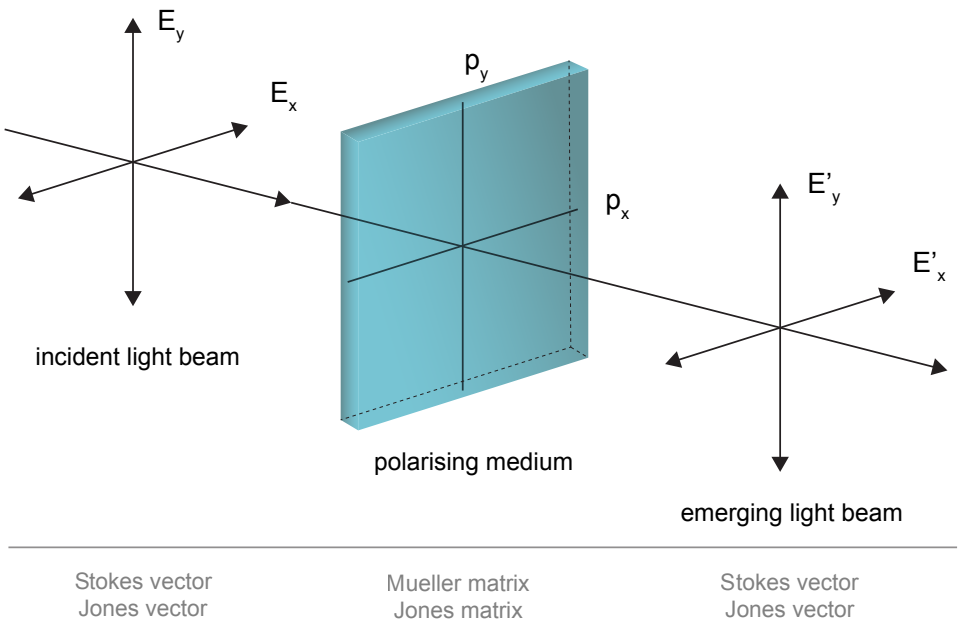

Figure 1.3: Diagram showing an incident light beam propagating through a polarising medium. Notes under the line shows possible mathematical representation. The resulting polarisation of the emerging light is found taking the product of the Mueller (or Jones) matrix of the optical element and the Stokes (or Jones) vector of the incident light. [21]

medium. There are following types of surfaces:

- Perfectly diffuse – act as a depolarisers, any polarisation that is present in the incident light is destroyed
- Perfectly smooth – Fresnel reflection coefficients give a full description and an exact solution for light and its polarisation state behaviour, see section 1.7
- Glossy – various approximations have to be used (Torrance-Sparrow, He-Torrance-Sillion-Greenberg, Weidlich-Wilkie BRDF models)

1.2.3 Mathematical Description of Polarised Light

Several mathematical systems have been developed to deal with polarisation problems in optics. The two of them, which are used in this master thesis are the 4-dimensional Mueller calculus and the 2-dimensional Jones calculus. Both these systems describe the light as a vector and the effect of the optical medium on the light as a transformation matrix (see Fig. 1.3).

The Jones matrix formalism involves complex quantities and is the most appropriately used when the separation of the real and imaginary parts is needed or when the light amplitudes must be superposed. Jones calculus, comparing to the Mueller calculus, is limited to treating only completely polarised light, it cannot describe partly polarised or unpolarised light. Each Jones matrix can be converted into a corresponding Mueller matrix.

The Mueller calculus involves real quantities and serves the best for intensity superposition problems.

Each calculus must have its coordinate system stated.

The following text is organized as follows: The coordinate system is discussed in the next section 1.3. The Mueller calculus is described in the section 1.4, the Jones calculus in 1.5 and one of the possible conversions of the Jones to Mueller calculus can be found in 1.6.

1.3 Coordinate Systems and Basis

Both Jones and Mueller calculus depend on the definition of the coordinate system. If the coordinate is rotated by some angle, the vectors and matrices will become different.

Figure 1.4 shows the unit hemisphere above a reflecting surface, which is used to describe the direction of incidence I and the direction of reflection R. Let's define an incident plane to be the plane containing the global surface normal vector N and the incoming direction I (highlighted in yellow color), the reflected plane to be the plane containing the global surface normal vector N and the reflected direction R (highlighted in blue color), and scattering plane to be the plane that contains the incoming direction I and the reflected direction R (highlighted in green color).

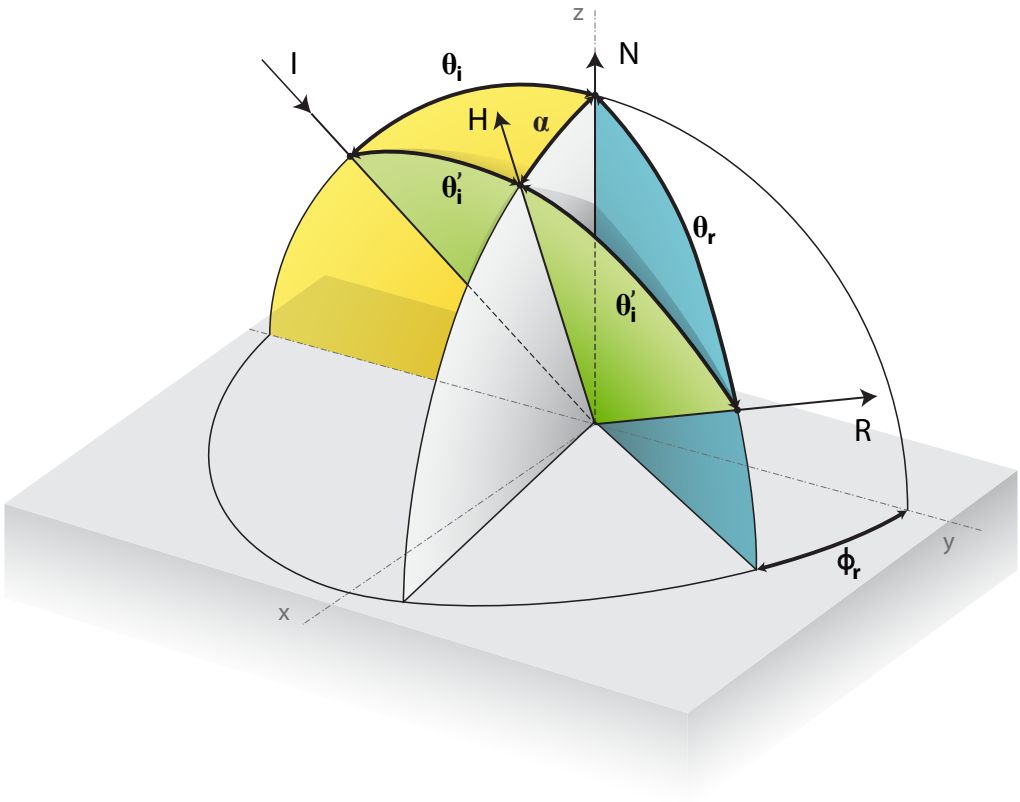

Figure 1.4: Spatial angles of incident and reflected radiance

The incoming direction I is specified by its zenith angle θ_i measured from the surface normal N. The direction of the reflected light R requires specification of two angles: the zenith angle θ_r measured from the surface normal N and the azimuthal angle ϕ_r measured from the plane of incidence. When $\phi_r = 0$, the incident, reflected, and scattering planes are all the same thing. When $\pi > \phi_r > 0$, we are considering light reflected to the left of the incident plane, and when $-\pi < \phi_r < 0$, we are considering light reflected to the right of the incident plane.

The last vector H (known as a halfway vector) is the angular bisector of the incoming direction I and the reflected direction R and it represents the normal of the facets that the surface is composed of. The facet normals are inclined at an angle α with respect to the normal of the mean surface N. The angle θ_i' defines the angle of incidence with respect to the facets and due to the perfect specularity of facets, the reflectance angle θ_i' is the same as the incident angle.

The angles θ_i', α are related to θ_i, θ_r, ϕ_r by the following relations [15]:

$$\begin{aligned} \theta_i' &= \frac{1}{2}\cos^{-1}\left(\cos\theta_r\cos\theta_i - \sin\theta_r\sin\theta_i\cos\phi_r\right) \\ \alpha &= \cos^{-1}\left(\cos\theta_i\cos\theta_i' + \sin\theta_i\sin\theta_i'\cos\beta\right) \\ \textit{where} & \\ \beta &= \sin^{-1}\left(\frac{\sin\phi_r\sin\theta_r}{\sin 2\theta_i'}\right) \end{aligned} \tag{1.3}$$

In the plane of incidence, Eqs. 1.3 simplify to

$$\begin{aligned} \theta_i' &= \frac{(\theta_i + \theta_r)}{2} \\ \alpha &= \frac{(\theta_r - \theta_i)}{2} \end{aligned} \tag{1.4}$$

1.3.1 Basis

To state a coordinate system, a basis must be defined. A basis is a set of linearly independent vectors, which defines a vector's orientation. In this thesis, we are interested in following two basis sets:

- s-p basis
- scattering basis

1.3.2 s-p Basis

The s-p basis set is given by two planes defined by the incident beam I and reflected beam R, respectively, with the surface normal N. It is suitable, e.g. for calculating scattering mechanisms.

1.3.3 Scattering Basis

The scattering basis is defined by a single plane containing the incident and reflected beams with the facet normal (halfway vector) H. If one defines the

basis to be with respect to the scattering plane, then, for the facet model, the Mueller matrix is in block diagonal form. Scattering basis is actually a useful basis for rendering applications, but it is not necessarily the best for other optical applications, or for calculating other scattering mechanisms.

1.3.4 Glossy BRDF Models

All the Fresnel, Torrance-Sparrow, He-Torrance-Sparrow-Greenberg and Weidlich-Wilkie models report the scattering in an s-p basis. Hence, they have to perform the rotation to report in the scattering basis, which results in block diagonal version of Mueller matrices, which are more easily programmable as they contain zeros.

It is important to keep in mind, that in the specular geometry, there is no difference between the scattering plane coordinate system and the s-p coordinate system. The plane of incidence, the plane of reflection, and the scattering plane are all the same due to the Snell's law. For the Lambertian component, setting basis is trivial, because a Lambertian surface is totally depolarising. That is, Mueller Matrix of depolariser is the same in all coordinate systems.

Note: All the Mueller and Jones matrices are reported in scattering basis if it is not said otherwise.

1.3.5 Rotation Matrix

Vectors and matrices can be rotated into another basis by the rotation matrix. Rotation matrix R is a matrix used to perform a rotation in Euclidean space. Rotation matrices are square orthogonal matrices with real entries and with determinant equal to 1, defined as [24]:

$$R^T = R^{-1} \tag{1.5}$$

thus

$$R^T * R^{-1} = 1 \tag{1.6}$$

Jones vector, respectively Stokes vector can be rotated by some angle ψ into another basis by the rotation matrix R_J

$$\mathrm{R}_J = \begin{bmatrix} \cos(\psi) & -\sin(\psi) \\ \sin(\psi) & \cos(\psi) \end{bmatrix}, \tag{1.7}$$

respectively R_S

$$\mathrm{R}_J = \begin{bmatrix} 1 & 0 & 0 & 0 \\ 0 & \cos(2\psi) & -\sin(2\psi) & 0 \\ 0 & \sin(2\psi) & \cos(2\psi) & 0 \\ 0 & 0 & 0 & 1 \end{bmatrix}. \tag{1.8}$$

Jones and Mueller matrices can be rotated similarly, but one needs to keep in mind that the bases for the incident and reflected directions may be different. Matrix, A, simply maps one vector, x, to another, y. This can be expressed as

$$y = A \cdot x \tag{1.9}$$

The basis for vector x can be changed by inserting a rotation matrix R_1:

$$y = A \cdot R_1^T \cdot R_1 \cdot x \tag{1.10}$$

Basis for the y vector can be changed with another rotation matrix R_2:

The basis for vector x can be changed by inserting a rotation matrix R_1:

$$R_2 \cdot y = R_2 \cdot A \cdot R_1^T \cdot R_1 \cdot x \tag{1.11}$$

This can be rewritten as

$$(R_2 \cdot y) = (R_2 \cdot A \cdot R_1^T) \cdot (R_1 \cdot x), \tag{1.12}$$

thus, in the new bases for x and y the matrix relating $R_2 \cdot y$ to $R_1 \cdot x$ is $R_2 \cdot A \cdot R_1^T$.

1.4 Mueller Matrix Calculus

The Mueller matrix calculus was introduced by Hans Mueller in 1943. [3] [25] In this technique, the effect of the optical medium is represented by a 4x4 matrix called the Mueller matrix. The calculus uses Stokes vectors to represents polarised, partially polarised or unpolarised light.

1.4.1 Stokes Vectors

The Stokes vector S denotes a group of four measurable parameters that completely describe the polarisation state of a given light (i.e. fully, partially or unpolarised light) and serves as a data structure for storing light information.

The individual parameters are referred to as Stokes components S_i, where $i = 0, 1, 2, 3$. The first parameter expresses the total intensity of the light. The parameter S_1 describes the amount of linear horizontal or vertical polarisation, the parameter S_2 describes the amount of linear polarisation rotated by 45° and the remaining parameter S_3 describes the amount of right or left circular polarisation contained within the beam. Stokes Vectors are real quantities and while the first parameter is obviously always positive, the remaining parameters are bounded by $[-S_0, S_0]$. Fig. 1.5 gives a graphical representation of the individual Stokes components.

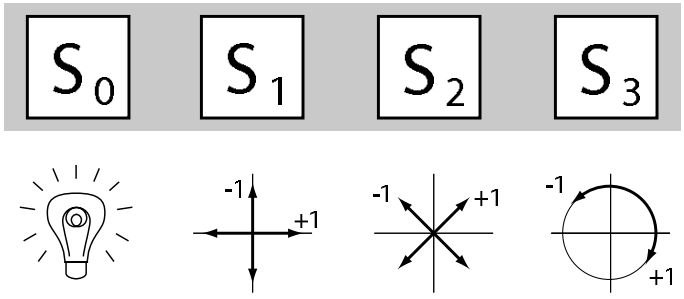

Figure 1.5: Graphical representationof the Stokes components. Image courtesy of [2].

Mathematically this can be summarized as

$$\begin{aligned} S_0 &= E_x E_x^* + E_y E_y^* \\ S_1 &= E_x E_x^* - E_y E_y^* \\ S_2 &= E_x E_y^* + E_y E_x^* \\ S_3 &= i(E_x E_y^* - E_y E_x^*) \end{aligned} \tag{1.13}$$

which is a complex representation of Stokes components (chapter 4.2 of [3]). The parameters S_1, S_2 and S_3 are under the following constraint:

$$S_0^2 \geq \sqrt{S_1^2 + S_2^2 + S_3^2} \tag{1.14}$$

The equality sign applies when the light is completely polarised, and the inequality sign in the case of partially polarised light or unpolarised.

An important quantity describing various polarisation conditions is the degree of polarisation P, which is of form

$$P = \frac{I_p ol}{I_t ot} = \frac{\sqrt{S_1^2 + S_2^2 + S_3^2}}{S_0}, \qquad 0 \leq P \leq 1 \tag{1.15}$$

Thus, $P = 0$ when the light is unpolarised, $P = 1$ when the light is completely polarised and $0 \leq P \leq 1$ when the light is partially polarised.

The Stokes components can be arranged in a column matrix and written as

$$S = \begin{pmatrix} S_0 \\ S_1 \\ S_2 \\ S_3 \end{pmatrix} \tag{1.16}$$

.

1.4.2 Mueller Matrix

We do not only need a data structure to store light information, but also a data structure to represent the optical medium describing the light alteration. When an optical beam interacts with a surface, its polarisation state is almost always changed according to the type of the surface by changing the amplitude(s), the phase, by rotating the ellipse or by transferring energy from polarised state to the unpolarised state. Further description about surface types is provided in section 1.2.2.

Here's a list of optical elements and the type of change they cause:

- Polarizer (diattenuator) – changes the amplitudes
- Retarder (wave plate) – causes phase shift
- Rotator – rotates the orthogonal components of the electric field
- Depolariser – depolarises light

The package describing these optical devices is called a Mueller matrix. A Mueller matrix describes all changes that the intensity and polarisation state of incident light can be subjected to.

A Mueller matrix M has the general form of

$$M = \begin{pmatrix} m_{11} & m_{12} & m_{13} & m_{14} \\ m_{21} & m_{22} & m_{23} & m_{24} \\ m_{31} & m_{32} & m_{33} & m_{34} \\ m_{41} & m_{42} & m_{43} & m_{44} \end{pmatrix}. \tag{1.17}$$

It is a 4x4 matrix containing 16 elements, which are real quantities. Let the incident beam is characterized by its Stokes parameters S_i, where $i = 0, 1, 2, 3$. The incident optical beam interacts with a polarising medium, and the emerging beam is characterized by a new set of Stokes parameters S'_i, where again $i = 0, 1, 2, 3$. The emerging beam S'_i can be expressed as a linear combination of the four Stokes parameters of the incident beam S_i by the relations

$$\begin{aligned} S'_0 &= m_{11}S_0 + m_{12}S_1 + m_{13}S_2 + m_{14}S_3 \\ S'_1 &= m_{21}S_0 + m_{22}S_1 + m_{23}S_2 + m_{24}S_3 \\ S'_2 &= m_{31}S_0 + m_{32}S_1 + m_{33}S_2 + m_{34}S_3 \\ S'_3 &= m_{41}S_0 + m_{42}S_1 + m_{43}S_2 + m_{44}S_3 \end{aligned} \tag{1.18}$$

In matrix form

$$\begin{pmatrix} S'_0 \\ S'_1 \\ S'_2 \\ S'_3 \end{pmatrix} = \begin{pmatrix} m_{11} & m_{12} & m_{13} & m_{14} \\ m_{21} & m_{22} & m_{23} & m_{24} \\ m_{31} & m_{32} & m_{33} & m_{34} \\ m_{41} & m_{42} & m_{43} & m_{44} \end{pmatrix} \begin{pmatrix} S_0 \\ S_1 \\ S_2 \\ S_3 \end{pmatrix} \tag{1.19}$$

or

$$S' = M \cdot S \tag{1.20}$$

where S and S' are the Stokes vectors of the incident and emerging beam, respectively, and M is a Mueller matrix. (chapter 5.1 of [3])

A list of common types of Mueller matrices follows (chapter 3.3 in [2]).

Polariser (diattenuator)

Polariser is an optical element that changes the orthogonal amplitudes unequally. Let the components of the incident beam are represented by E_x and E_y. The components of the beam emerging from the polariser are represented by E'_x and E'_y, which are parallel to the original axes. The fields are related by

$$E'_x = p_x E_x \qquad 0 \leq p_x \leq 1 \tag{1.21}$$

$$E'_y = p_y E_y \qquad 0 \leq p_y \leq 1 \tag{1.22}$$

where p_x and p_y are the amplitude attenuation coefficients along orthogonal transmission axes.

Mueller matrix for a polariser with amplitude attenuation coefficients p_x and p_y is of a standard form

$$\mathrm{M}_{pol} = \frac{1}{2}\begin{bmatrix} p_x^2 + p_y^2 & p_x^2 - p_y^2 & 0 & 0 \\ p_x^2 - p_y^2 & p_x^2 + p_y^2 & 0 & 0 \\ 0 & 0 & 2p_x p_y & 0 \\ 0 & 0 & 0 & 2p_x p_y \end{bmatrix} \tag{1.23}$$

For $p_x = p_y = p$ we gain the plain attenuation. It describes an idealised interaction, where light interacts with matter without changing its polarisation state, but the intensity of the incident beam is reduced by a factor of p^2. The corresponding Mueller matrix has the following form:

$$\mathrm{M}_{att} = p^2 \begin{bmatrix} 1 & 0 & 0 & 0 \\ 0 & 1 & 0 & 0 \\ 0 & 0 & 1 & 0 \\ 0 & 0 & 0 & 1 \end{bmatrix} \tag{1.24}$$

Retarder (phase shifter)

Retarder is an optical element which introduces the phase shift of ϕ between the orthogonal components of an optical beam. The standard Mueller matrix for the retarder is given by

$$\mathrm{M}_{ret} = \begin{bmatrix} 1 & 0 & 0 & 0 \\ 0 & 1 & 0 & 0 \\ 0 & 0 & \cos\phi & \sin\phi \\ 0 & 0 & -\sin\phi & \cos\phi \end{bmatrix} \tag{1.25}$$

It can be seen that for an ideal retarder there is no loss in intensity.

Depolariser

When an incident beam interacts with a perfectly diffuse surfaces or transmissive materials, the light intensity is attenuated to some degree, but any polarisation that is present in the incident beam is destroyed as these surfaces act as depolarisers. For an attenuation factor of p, the depolariser has the following form:

$$\mathrm{M}_{dep} = p \begin{bmatrix} 1 & 0 & 0 & 0 \\ 0 & 0 & 0 & 0 \\ 0 & 0 & 0 & 0 \\ 0 & 0 & 0 & 0 \end{bmatrix} \tag{1.26}$$

ABCD Mueller Matrix

The form of M_{pol} and M_{ret} suggest that the matrices can be represented by a single matrix. This matrix is called ABCD or diagonal block polarisation matrix and it is of form

$$\mathrm{M}_{ABCD} = \begin{bmatrix} A & B & 0 & 0 \\ B & A & 0 & 0 \\ 0 & 0 & C & D \\ 0 & 0 & -D & C \end{bmatrix}, \tag{1.27}$$

where for polariser:

$$\begin{aligned} A &= \frac{1}{2}(p_x^2 + p_y^2) \\ B &= \frac{1}{2}(p_x^2 - p_y^2) \\ C &= \frac{1}{2}(2p_x p_y) \\ D &= 0 \end{aligned} \tag{1.28}$$

and for retarder:

$$\begin{aligned} A &= 1 \\ B &= 0 \\ C &= \cos\phi \\ D &= \sin\phi \end{aligned} \tag{1.29}$$

By multiplying 1.23 and 1.25 we will obtain another matrix that can be represented by an ABCD matrix.

Mueller Matrix Algebra

The main rules used in performing adding and multiplications are the standard rules of matrix algebra.

If we shine light of some polarisation simultaneously onto more samples with different Mueller matrices denoted as M_i where $i = 1, 2, ...$, it is often advantageous to combine a given series of matrices into a single one, which is called the matrix of train, M_{train}. M_{train} is computed simply by multiplication as follows

$$M_{train} = M_i \cdot M_{i-1} \cdot ... \cdot M_1 \tag{1.30}$$

1.5 Jones Matrix Calculus

Jones calculus was discovered by R. C. Jones in 1941. [21] It represents another way how to mathematically describe polarised light. Similarly to Mueller calculus, it represents light using Jones vectors and the surface by a Jones matrix. The following text provides only a brief introduction to Jones calculus. For further information refer to [3].

1.5.1 Jones Vector

Jones formalism uses complex, two element Jones vector E to describe the light polarisation. The vector describes the amplitude and phase of the light[3], [22], i.e.

$$E = \begin{pmatrix} E_x \\ E_y \end{pmatrix} = \begin{pmatrix} E_{0_x} e^{i\delta_x} \\ E_{0_y} e^{i\delta_y} \end{pmatrix} \tag{1.31}$$

where E_{0_x} and E_{0_y} are the amplitudes, δ_x and δ_y are the phases and i represents imaginary unit.

1.5.2 Jones Matrix

The Jones matrix describes the relationship between two complex amplitudes of Jones vector of the incident wave with two complex amplitudes of the outgoing wave. This relation is written as

$$\begin{aligned} E'_x &= j_{11}E_x + j_{12}E_y \\ E'_y &= j_{21}E_x + j_{22}E_y \end{aligned} \tag{1.32}$$

where E'_x and E'_y are the components of the emerging beam and E_x and E_y are the components of the incident beam. The quantities j_{ik} where $i, k = 1, 2$ are the transforming elements of the transformation Jones matrix. It can be written as (the following text was taken from [3], chapter 11)

$$\begin{pmatrix} E'_x \\ E'_y \end{pmatrix} = \begin{pmatrix} j_{11} & j_{12} \\ j_{21} & j_{22} \end{pmatrix} \begin{pmatrix} E_x \\ E_y \end{pmatrix} \tag{1.33}$$

or

$$E' = JE \tag{1.34}$$

where

$$J = \begin{pmatrix} j_{11} & j_{12} \\ j_{21} & j_{22} \end{pmatrix} \tag{1.35}$$

where J is a 2x2 matrix and is called Jones matrix.

1.6 Jones-Mueller Matrix Conversion

For each Jones matrix, a corresponding Mueller matrix exists. One of the formalisms for converting Jones to Mueller matrix is described in Appendix C in [3].[2]

The Mueller matrix elements in terms of Jones matrix J elements are:

$$\begin{aligned} m_{11} &= (j_{11}j_{11}^* + j_{12}j_{12}^* + j_{21}j_{21}^* + j_{22}j_{22}^*)/2 \\ m_{12} &= (j_{11}j_{11}^* + j_{21}j_{21}^* - j_{12}j_{12}^* - j_{22}j_{22}^*)/2 \\ m_{13} &= (j_{12}j_{11}^* + j_{22}j_{21}^* + j_{11}j_{12} + j_{21}j_{22}^*)/2 \\ m_{14} &= i(j_{12}j_{11}^* + j_{22}j_{21}^* - j_{11}j_{12}^* - j_{21}j_{22}^*)/2 \\ m_{21} &= (j_{11}j_{11}^* + j_{12}j_{12}^* - j_{21}j_{21}^* - j_{22}j_{22}^*)/2 \\ m_{22} &= (j_{11}j_{11}^* - j_{21}j_{21}^* - j_{12}j_{12}^* + j_{22}j_{22}^*)/2 \\ m_{23} &= (j_{11}j_{12}^* + j_{12}j_{11}^* - j_{21}j_{22}^* - j_{22}j_{21}^*)/2 \\ m_{24} &= i(j_{12}j_{11}^* + j_{21}j_{22}^* - j_{22}j_{21}^* - j_{11}j_{12}^*)/2 \end{aligned} \tag{1.36}$$

[2] The element m_{31} in the original text in [3] is incorrect. The correct version was found in SCATMECH library, Mueller.cpp source code [18].

$$
\begin{aligned}
m_{31} &= (j_{11}j_{21}^* + j_{21}j_{11}^* + j_{12}j_{22}^* + j_{22}j_{12}^*)/2 \\
m_{32} &= (j_{11}j_{21}^* + j_{21}j_{11}^* - j_{12}j_{22}^* - j_{22}j_{12}^*)/2 \\
m_{33} &= (j_{11}j_{22}^* + j_{12}j_{21}^* + j_{21}j_{12}^* + j_{22}j_{11}^*)/2 \\
m_{34} &= i(-j_{11}j_{22}^* + j_{12}j_{21}^* - j_{21}j_{12}^* + j_{22}j_{11}^*)/2 \\
m_{41} &= i(j_{11}j_{21}^* + j_{12}j_{22}^* - j_{21}j_{11}^* - j_{22}j_{12}^*)/2 \\
m_{42} &= i(j_{11}j_{21}^* - j_{12}j_{22}^* - j_{21}j_{11}^* + j_{22}j_{12}^*)/2 \\
m_{43} &= i(j_{11}j_{22}^* + j_{12}j_{21}^* - j_{21}j_{12}^* - j_{22}j_{11}^*)/2 \\
m_{44} &= (j_{11}j_{22}^* - j_{12}j_{21}^* - j_{21}j_{12}^* + j_{22}j_{11}^*)/2
\end{aligned}
\tag{1.37}
$$

A reversed conversion, i.e from Mueller to Jones matrix, is also possible. However, since the Jones matrix can't represent a depolariser or scatterer, the information on depolarisation contained in the Mueller matrix must be discarded.

1.7 Perfectly Smooth Surfaces – The Fresnel Terms

The interaction of light beam with a perfectly smooth phase boundaries can be mathematically expressed by a widely known set of equations called Fresnel terms or Fresnel reflection coefficients. Fresnel terms predict correctly the magnitude of the reflected and transmitted intensities of an optical beam.

Suppose we have a light beam travelling from a homogeneous medium of a given refractive index n_1 in the incoming direction I at an angle θ_i. Its electric field can be decomposed into two orthogonal components, E_x and E_y (see Eqs. 1.1 and 1.2). The electric field vector of E_x and E_y is parallel, respectively perpendicular to the plane of incidence. This behaviour is illustrated in Figure 1.6. Note that E_y points to the plane of paper.

The light encounters an interface with another homogeneous medium of a different refractive index n_2. Usually part of the light is reflected in the direction of R at an angle θ_r and part is refracted in the direction of T at an angle θ_t. The relation between angles θ_i, θ_r and θ_t is given by the law of reflection:

$$\theta_i = \theta_r \tag{1.38}$$

and the Snell's law:

$$\frac{\sin\theta_i}{\sin\theta_r} = \frac{n_2}{n_{1.}} \tag{1.39}$$

The fraction of reflected/transmitted light is dependent upon θ_i and incident light polarisation state and can be calculated using the Fresnel equations for reflection and transmission.

1.7.1 Special Angles

There are two special angles that should be considered, Brewster's angle and the critical angle. An angle is called the Brewster's angle θ_{i_B} when $\theta_i + \theta_t = 90°$. For Brewster's angle, the reflected amplitude for the light polarised parallel to the incident plane vanishes to zero. [3], [27] The Brewster's angle θ_B is defined as

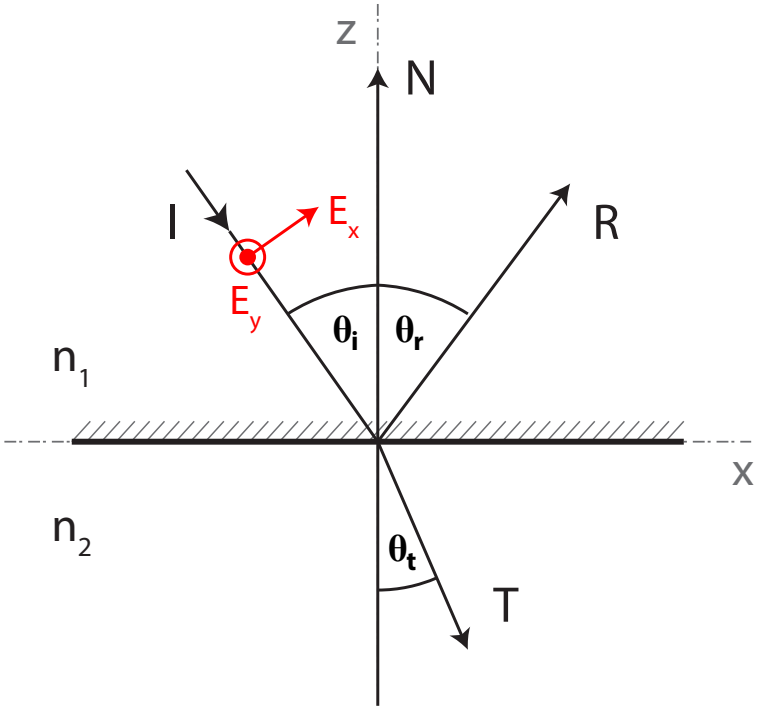

Figure 1.6: A diagram showing a light beam going from a lower index medium to a higher index medium.

$$\theta_{i_B} = \tan\left(\frac{n_2}{n_1}\right). \tag{1.40}$$

The critical angle θ_{i_c} is such an angle of incidence above for which a phenomenon known as total internal reflection (TIR) occurs. That is, if n_1 is lower than n_2 and the incidence angle is greater or equal to the cricital angle, the light cannot passes through and is entirely reflected. [3], [28]

The critical angle is defined as

$$\theta_{i_c} = \arcsin\left(\frac{n_2}{n_1}\right). \tag{1.41}$$

1.7.2 The Fresnel Terms

In their most extensive form, the Fresnel terms consist of two pairs of equations. The first pair F_s, F_p determines the amount of incident light intensity, which is reflected for the perpendicular and parallel components of the incident light in relation to the plane of incidence. The second pair δ_s, δ_p describes the retardance (phase-shift) that the incident light is subjected to, i.e. the relative phase shift that the vertical and horizontal components of the light undergo during reflection. Retardance is essential for polarising renderer, as i.e. the phenomena like the conversion of linearly polarised incident light into elliptically polarised reflected light, which can occur on metallic surfaces, is caused by a phase shift that happen during reflection. [2]

The Fresnel reflectance coefficients are of following forms:

$$
\begin{aligned}
F_s(\theta_i, \eta) &= \frac{a^2 + b^2 - 2a\cos\theta_i + \cos^2\theta_i}{a^2 + b^2 + 2a\cos\theta_i + \cos^2\theta_i} \\
F_p(\theta, \eta) &= \frac{a^2 + b^2 - 2a\sin\theta_i\tan\theta_i + \sin^2\theta_i\tan^2\theta_i}{a^2 + b^2 + 2a\sin\theta_i\tan\theta_i + \sin^2\theta_i\tan^2\theta_i} F_s(\theta, \eta) \\
\tan\delta_s &= \frac{2b\cos\theta_i}{\cos^2\theta_i - a^2 - b^2} \\
\tan\delta_p &= \frac{2\cos\theta_i[(n^2 - k^2)b - 2nka]}{(n^2 + k^2)^2\cos^2\theta_i - a^2 - b^2} \\
&with \\
\eta &= n + ik \;\; (the\ complex\ IOR) \\
2a^2 &= \sqrt{(n^2 - k^2 - \sin^2\theta_i)^2 + 4n^2k^2} + n^2 - k^2 - \sin^2\theta_i \\
2b^2 &= \sqrt{(n^2 - k^2 - \sin^2\theta_i)^2 + 4n^2k^2} - n^2 + k^2 + \sin^2\theta_i
\end{aligned}
\tag{1.42}
$$

The angle θ_i is the incident angle at which the Fresnel coefficients are evaluated. The parameter $\eta = n - \kappa$ is the complex index of refraction for the material surface, where n is the index of refraction and κ is the coefficient of extinction, where

$$
\begin{aligned}
\kappa = 0 \qquad & \text{for dielectrics} \\
else \qquad & \text{for conductors}
\end{aligned}
\tag{1.43}
$$

The intensity of the transmission along the refracted ray T is also applied to both perpendicular and parallel and it is defined as the following:

$$
\begin{aligned}
T_s &= 1 - F_s \\
T_p &= 1 - F_p
\end{aligned}
\tag{1.44}
$$

The list of Fresnel equations is followed by their graphical representation plotted in charts for three typical scenarios – dielectric from outside, from inside and conductor.

Dielectric – External Reflection

The curves that can be seen in figures 1.7, 1.8, 1.9 are the graphical representation of the Fresnel reflection for a typical dielectric substance with an index of refraction $n_2 = 1.5$ (glass). The outside medium is an air with an index of refraction $n_1 = 1$.

Note that the reflected amplitude for the parallel polarized light in figure 1.7 is zero for the Brewster angle. The reflected light is then linearly polarized in a plane perpendicular to the incident plane. [27]

Figure 1.9 shows Fresnel retardance, which causes a phase changes. One can see that the interface causes a linear polarisation over the entire range of incident angles θ_i, and only induces phase shift between the incident light components or either beneath the Brewster's angle or above.

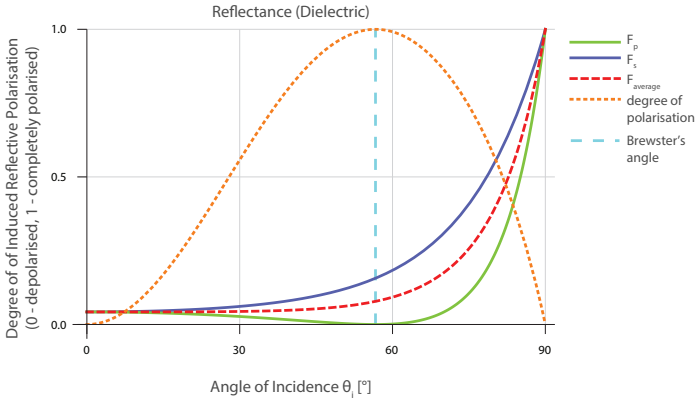

Figure 1.7: Amplitude reflection coefficients versus incidence angle for external reflection on dielectric for $n_1 = 1$ and $n_2 = 1.5$. Image courtesy of [2].

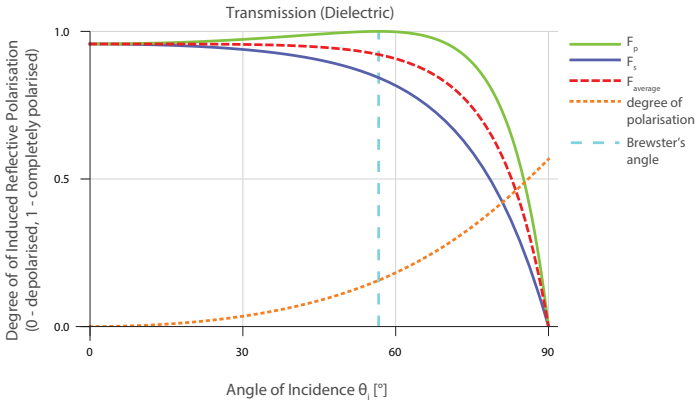

Figure 1.8: Amplitude reflection coefficients versus incidence angle for external transmission on dielectric for $n_1 = 1$ and $n_2 = 1.5$. Image courtesy of [2].

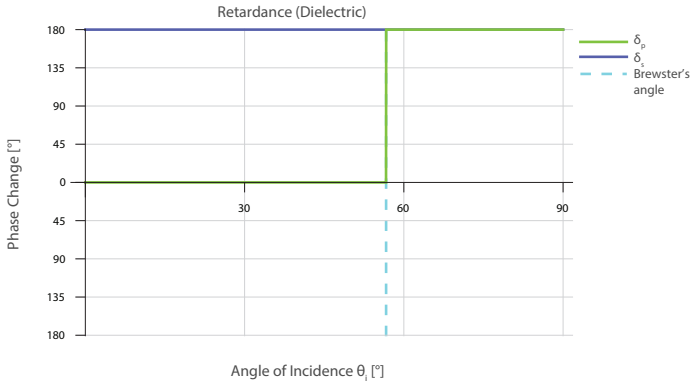

Figure 1.9: Phase changes for external reflection versus incidence angle for $n_1 = 1$ and $n_2 = 1.5$. Image courtesy of [2].

Dielectrics from inside

Figures 1.10, 1.11, 1.12 illustrate a scenario, where light is leaving a dielectric with an index of refraction $n_2 = 1.5$ to a less dense medium with an index of refraction $n_1 = 1$. Up to the total internal reflection, the interface behaves like a normal reflective interface: it linearly polarises reflected light, and induces a phase shift of either π or 0. In the area of total internal reflection above that angle, though, light is perfectly reflected and no linear polarisation is induced. But note that for total internal reflection angles, the interface is capable of inducing a non-integer phase shift between the incident wave-train components! (cited from [2]).

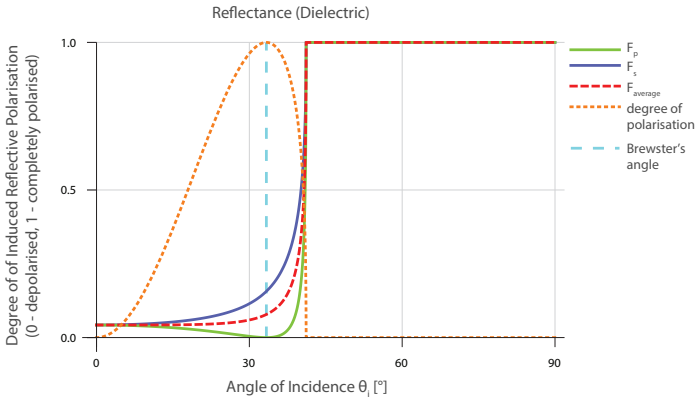

Figure 1.10: Amplitude reflection coefficients versus incidence angle for internal reflection on dielectric for $n_1 = 1$ and $n_2 = 1.5$. Image courtesy of [2].

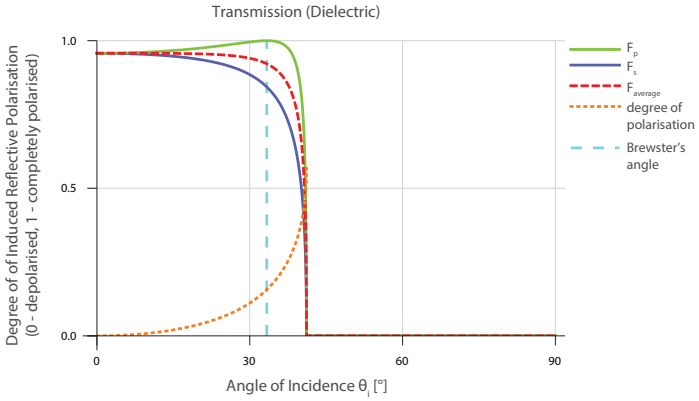

Figure 1.11: Amplitude reflection coefficients versus incidence angle for internal transmission on dielectric for $n_1 = 1$ and $n_2 = 1.5$. Image courtesy of [2].

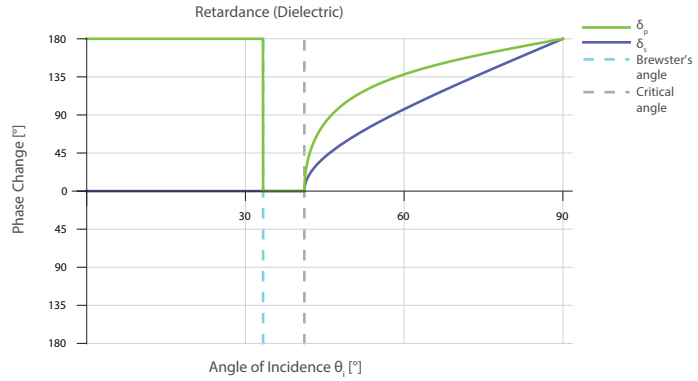

Figure 1.12: Phase changes for internal reflection versus incidence angle for $n_1 = 1$ and $n_2 = 1.5$. Image courtesy of [2].

Conductors

The third scenario shows the light behaviour on a typical conductor with a complex index of refraction η. The plot showing transmission is missing due to the fact that there is no macroscopically relevant transmission through a conductor as it is opaque.

The overall reflectance is much higher, that linear polarisation of reflected light is comparatively weak, and that over the entire range of reflection angles a non-integer phase shift is induced (cited from [2])

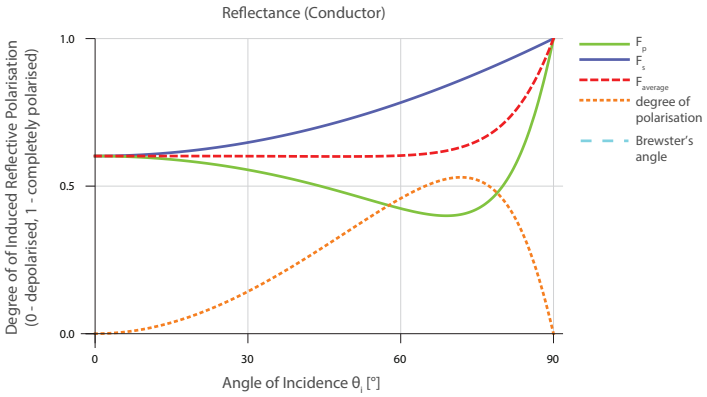

Figure 1.13: Amplitude reflection coefficients versus incidence angle on conductor for $n_1 = 1$ and η. Image courtesy of [2].

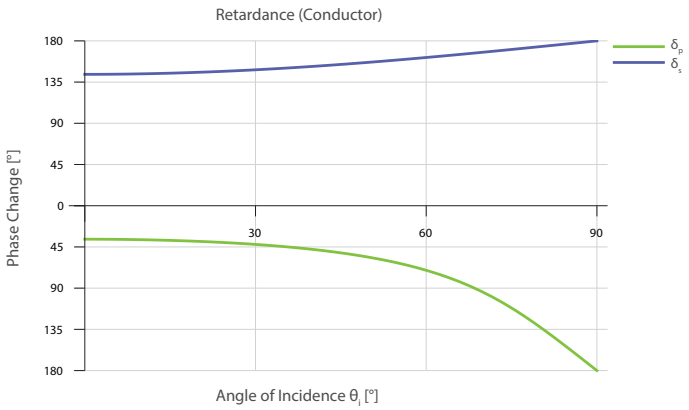

Figure 1.14: Phase changes for external reflection versus incidence angle on conductor for $n_1 = 1$ and η. Image courtesy of [2].

1.7.3 Mueller Matrix of Fresnel Reflectance

Fresnel reflection off of a perfectly specular surface is one of the two corner cases of reflectance, where an exact formulas for the resulting Mueller Matrix is already available (the second case is a perfect depolarised represented by Lambertian surface). The derivation of the Mueller matrix for Fresnel reflectance can be found in [3]. The Mueller matrix of Fresnel, M_F, in scattering basis is defined as

$$\mathrm{M}_F = \begin{bmatrix} A & B & 0 & 0 \\ B & A & 0 & 0 \\ 0 & 0 & C & S \\ 0 & 0 & -S & C \end{bmatrix}, \tag{1.45}$$

with

$$\begin{aligned} A &= \frac{F_s + F_p}{2} \\ B &= \frac{F_s - F_p}{2} \\ C &= \cos(\delta_s - \delta_p) \cdot \sqrt{F_s \cdot F_p} \\ S &= \sin(\delta_s - \delta_p) \cdot \sqrt{F_s \cdot F_p} \end{aligned}, \tag{1.46}$$

where the $\delta_s - \delta_p$ term is the total retardance the incident wave-train is subjected to.

1.7.4 Jones Matrix of Fresnel Reflectance

The Jones Matrix for Fresnel reflection in scattering plane is of form [17]

$$\mathrm{J}_F = \begin{bmatrix} F_s & 0 \\ 0 & F_p \end{bmatrix} \tag{1.47}$$

2. State of the Art

With increasing demands in science and entertainment industry, it is not surprising that computer graphics is one of the fastest growing industry in the world and that it is going through a rapid and strong development. The demands are obvious – the computer graphics should be indistinguishable from the real world.

To achieve this goal, it is essential to represent the appearance of objects (materials) according to reality, that is, to accurately simulate the behaviour of the light, when it shines on a surface of an object. That can be mathematically defined by the bidirectional reflectance distribution function (BRDF), which has proven its efficiency to describe complex light interaction with surfaces and in creating realistic illumination of the virtual world.

The content of this chapter is organized as follows – section 2.1 describes how the light flow throughout the scene is calculated, section 2.2 describes the bidirectional reflectance distribution function and section 2.3 provides an introduction to and also a motivation for rendering including the light polarisation phenomenon.

2.1 Rendering

Rendering is a process of creating an image of a synthetic scene from a mathematical model describing the scene. The model includes information about

- Light sources (defines where they are placed, of what type they are, ect.)
- Geometry (defines where in the scene each object is)
- Material (defines the interaction of the light with matter using Bidirectional Reflectance Distribution Function)
- Camera (defines where do we look into the scene from)

2.1.1 Rendering Equation

To be able to render realistic computer graphics, we have to know the amount and the distribution of light that reaches the camera from a given direction (i.e. through a given pixel). The light behaviour simulation is essential for the whole process of rendering. When an optical beam hits a point on a surface, it might be reflected, absorbed or refracted. There also can be additional light source at the point which emits light, or there can be additional light coming from another point on the surface. [8] The flow of light throughout a scene is a described by the rendering equation. [9] Solving rendering equation is the primary challenge of physically based rendering.

The rendering equation in angular form has the following form:

$$L_o(x, \omega_o) = L_e(x, \omega_o) + \int_{\omega_i \in H(x)} L_o(r(x, \omega_i) - \omega_i) \cdot f_r(x, \omega_i \to \omega_o) \cdot \cos(\theta_i) d\omega_i \tag{2.1}$$

where x is a point in the scene, ω_o is the direction of the outgoing light beam, ω_i is the direction of the incoming light beam, $L_o(x, \omega_o)$ is the total radiance outgoing from the point x in ω_o direction, $L_e(x, \omega_o)$ is the emitted radiance (from light source) from the point x in ω_o direction, $r(x, \omega_i)$ is a function which returns such a point of the scene, from which the light beam came from (the incoming direction ω_i), $L_o(r(x, \omega_i), -\omega_i)$ is the radiance coming toward the point x from the incoming direction ω_i, $\cos(\theta_i)$ is an angle between the incoming light and the normal and represent the attenuation of the incoming light, and $f_r(x, \omega_i \rightarrow \omega_o)$ is the bidirectional reflectance distribution function (BRDF). [12].

2.1.2 Path Tracing

An algorithm used to approximate the numerical solution of the rendering equation is called path tracing. The concept of the algorithm is following.

For each pixel of the final image cast a ray throughout the scene. Trace the ray to find the nearest point of intersection with a surface. If the ray hits a light source, its emitted radiance is calculated and the ray is then casted randomly back throughout the scene with a probability corresponding to the reflection coefficient. Then the whole procedure is recursively repeated.

The basic form of path tracing is not used in practice in general. The traced path add a non zero value to the result only if we hit a light source. The probability of hitting the light source reduces with the size of the light source. In case the scene is illuminated by a point light only, the probability of hitting the light source is reduced to zero. There are two ways of solving this - the BRDF sampling and light source sampling. [13]

2.2 BRDF

In computer graphics, a lot of research effort is focused to representation of the material appearance. The objects look differently when viewed from different angles and when illuminated from different directions. How objects look is defined by the behaviour of the light, more precisely by the distribution of reflected light at the surface.

The bidirectional reflectance distribution function (BRDF) f_r serves for the mathematical description of the reflective characteristics of surface and it expresses the amount of the light ray will be reflected in a particular outgoing direction. It is a function of form [11]

$$f_r(\omega_i \rightarrow \omega_o) = \frac{dL_r(\omega_o)}{dE(\omega_i)} = \frac{dL_r(\omega_o)}{L_i(\omega_i) \cdot \cos(\theta_i) \cdot d\omega_i} \tag{2.2}$$

where ω_i and ω_o is the incoming and outgoing direction of the light, respectively, $dL_r(\omega_o)$ is reflected radiance in the outgoing direction ω_o, $dE(\omega_i)$ is irradiance that expresses how much light is incoming at a point on a surface from the incoming direction ω_i. $dE(\omega_i)1$ can be expressed as: [10]

$$dE(\omega_i) = L_i(\omega_i) \cdot \cos(\theta_i) \cdot d\omega_i \tag{2.3}$$

A diagram showing BRDF can be seen in Figure 2.1.

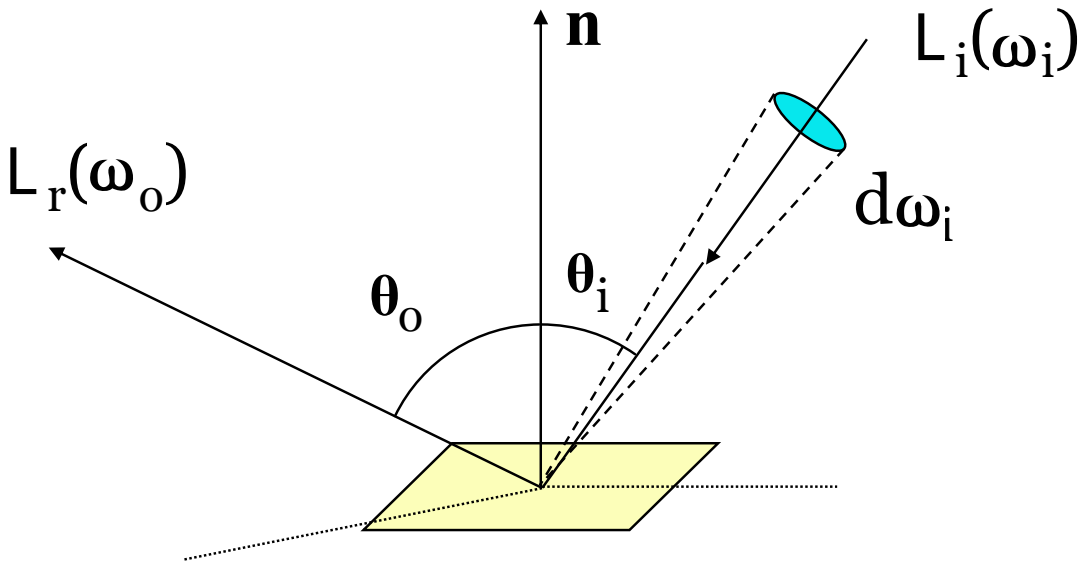

Figure 2.1: Diagram showing vectors used to define bidirectional reflectance distribution function visualisation. ω_i points towards the light source, ω_o points into the outgoing direction. Image courtesy of [14].

2.2.1 Types of BRDF

BRDF is a key component to deliver realistic surface reflectance behaviour.

The reflection can be divided into following three categories according to the type of surface (see Figure 2.2):

- Ideal diffuse (Lambertian)
- Ideal specular
- Glossy

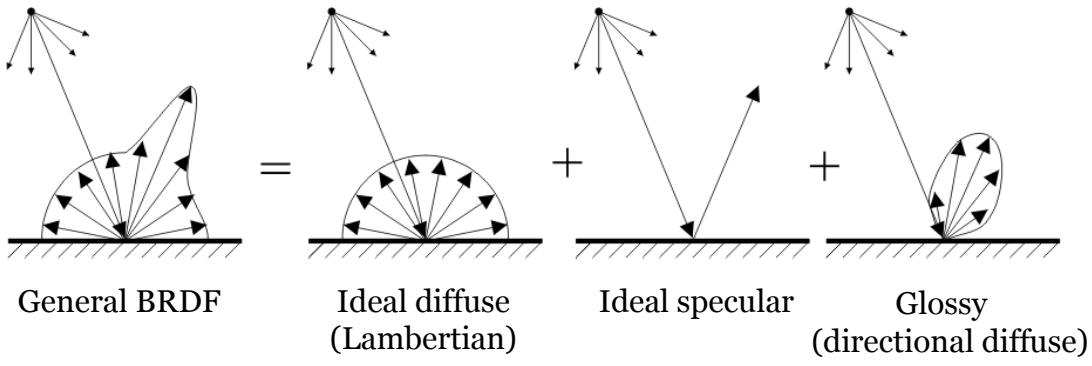

Figure 2.2: Types of BRDF. Image courtesy of [14].

When the light hits an ideal diffuse (Lambertian) surface, it is reflected equally into all directions. BRDF of ideal diffuse surfaces $f_{r,d}$ is constant.

$$f_{r,d}(x, \omega_i \rightarrow \omega_o) = f_{r,d}(x) \tag{2.4}$$

For the ideal specular surfaces the light is mirrored according to the laws of reflection. BRDF of ideal specular surfaces $f_{r,m}$ is of following form

$$f_{r,m}(\theta_i, \phi_i; \theta_o, \phi_o) = R(\theta_i) \frac{\delta(\cos\theta_i - \cos\theta_o))\delta(\phi_i - \phi_o \pm \pi)}{\cos\theta_i} \tag{2.5}$$

Both these just mentioned types of surface represent an extreme, which exists just in theory, not in the reality. The real objects' surface is something between ideal diffuse and ideal specular and the type is known as glossy. The rougher the surface is, the more dominant the diffuse component is, and vice versa with a smoother surface.

Computer graphics uses three approaches to simulate surface reflectance behaviour.

- Empirical
- Physically based
- Measurement of real surfaces and their approximation

Empirical models are often physically implausible, but their appearance results are reasonably good-looking at a moderate computational cost. Approximation of real surfaces measurement is problematic due to its acquisition costs. This approach is not analytical. The realistic surface reflectance behaviour is delivered by physically based reflectance models, which offer a great potential for creating convincing synthetic imagery. There are only few computer graphics suitable BRDF models, which are capable of describing polarising reflectance and.

These are:

- Fresnel
- Torrance-Sparrow
- He-Sillion-Torrance-Greenberg
- Weidlich-Wilkie layered model

These models will be the main subjects of investigation in this thesis.

2.3 Polarization Rendering

The technology for including polarisation in industrial-strength rendering engines is not entirely ready yet, despite the polarisation is one of the basic properties of the light. The reason seems to be logical. The effort-outcome ratio is poor, because the creation of such renderer would require to retrofit and re-design the entire conventional ray-based rendering system, namely:

- change of data structures used for light and attenuation
- implementation of a reference frame tracking for all paths that are traced

- implementation of a workflow that involves a polarisation capable image raw format
- replacement of all the BRDF and scattering models so that they yield the correct Mueller Matrix upon evaluation

which are just few of all the modifications that have to be made to achieve polarisation-capable renderer. Moreover, taking into account that human eye can't directly perceive most of these more subtle aspects of light, so that the polarisation changes on the resulting radiant intensity is quite negligible, it leads to a understandable decision to ignore polarisation property of light when rendering physically based images.

2.3.1 Where Polarisation Matters

Nevertheless, there are some exceptions, where polarisation matters and where it has the decisive influence on the overall appearance of the rendered scene. Scenes including multiple light bounces via specular surfaces are perhaps the most widely known area where polarisation matters. Rendering such scenes with and without taking polarisation into account exhibit visible differences. The reason of this is that the reflection from specular surfaces can both give rise to polarisation and alter an existing polarisation state. Mirror images of a glowing object also look different, when polarisation is taken into account, as well as in scenes where scattering interactions appear (atmospheric scattering).

Incorporating polarisation parameter into lighting model can enhance the physical realism of rendered images. It is directly useful in photography, where linear polarisation filters are commonly used to enhance or reduce specular reflection, but it would also find use in sophisticated engineering solutions such as the face or the material scanning set-ups ([4], [5]).

2.3.2 Advanced Rendering Toolkit

ART (Advanced Rendering Toolkit) is a predictive rendering research system under development at the computer graphics group at the Charles University, Prague, Czech Republic. [7] It provides command-line applications, which perform various tasks from photorealistic image synthesis field and it enables us to render photorealistic visual scenes. It is a rendering engine capable of rendering while taking the polarisation state of light into account.

ART will be used to test Mueller matrices, that will be derived in following chapters.

2.3.3 SCATMECH

SCATMECH in an object-oriented C++ class library developed by Thomas A. Germer at National Institute of Standards and Technology (NIST). [18] Amongst others, the library includes models for diffuse surface scattering that predict the BRDF, codes for calculating scattering by isolated particles, and codes for reflection, transmission, and diffraction from gratings. Emphasis has been given

to those diffuse scattering models which are physics-based and which predict the polarisation properties of the scattered light.

The reason, why we mention this library is that it is capable of evaluating Mueller matrix for Torrance-Sparrow model. However, its approach is different from ours. The way the Torrance-Sparrow model would be implemented with SCATMECH is not direct (there is actually no Torrance-Sparrow model in the library). Two sources need to be added together: a shadowed facet model and a Lambertian model. For the facet model, the Torrance-Sparrow shadow function would be chosen. Thus, SCATMECH just returns the numerical values of the Mueller matrix for Torrance-Sparrow model in a specified geometry and set of parameters, while our Mueller matrix evaluation upon this model will be analytical. The possibility to compare results is indeed useful.

3. Torrance-Sparrow Model

In 1967, K. E. Torrance and E. M. Sparrow presented a light reflection model by a rough surface, which successfully predicted the experimental findings of the real light waves behaviour. [15]

The basic concept of the model is provided in section 3.2 and in section 3.3 the Mueller matrix for this model is stated. The Torrance-Sparrow Mueller matrix testing results can be found in section 6.2.

3.1 The Coordinate System

To provide an easier orientation for the forthcoming formulas and angular notation, a diagram showing the coordinate system is again depicted in this section. The Figure 5.1 shows a diagram of spatial angles of incidence and reflected radiance. For more details, please refer to section 1.3.

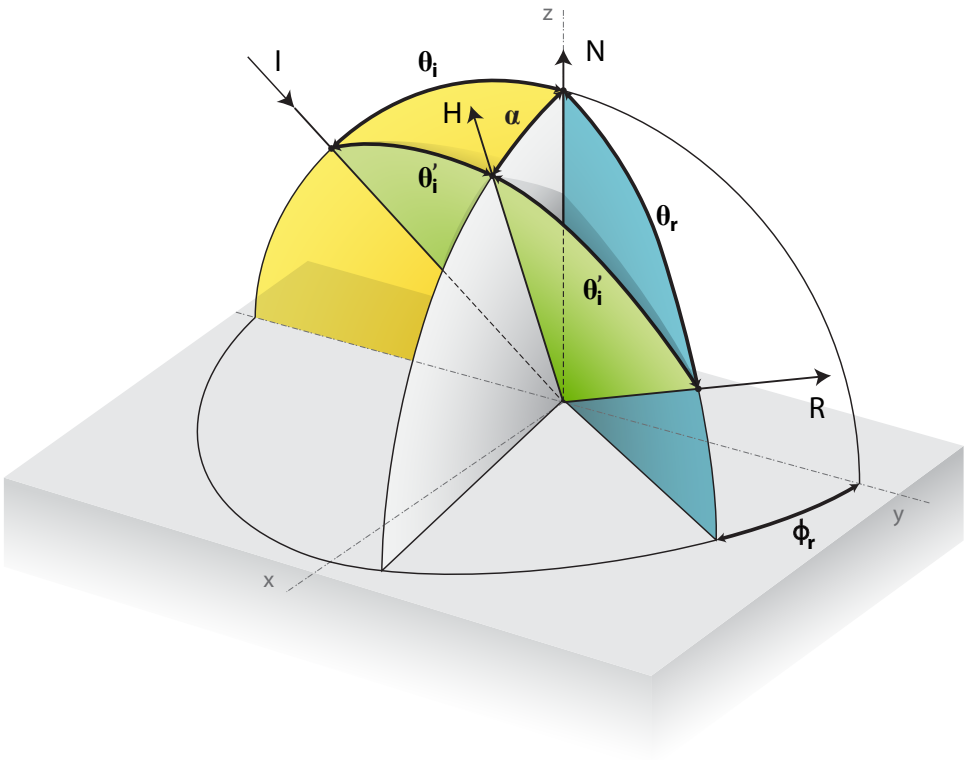

Figure 3.1: Spatial angles of incident and reflected radiance

3.2 Overview of the Model

The Torrance-Sparrow model is a micro-facet based model, which assumes that at a microscopic level of detail the surface consists of small, randomly disposed, perfectly specular planar facets.

The total reflection from a roughened surface is composed of two components – specular and diffuse. The specular component f_s consists of light waves that mirror-like reflect off of a single surface micro-facet. The diffuse component f_d consists of light waves that have had multiple reflections between micro-facets and/or penetrate into the outermost layer and then back to the surface (as it is sketched in Figure 3.2).

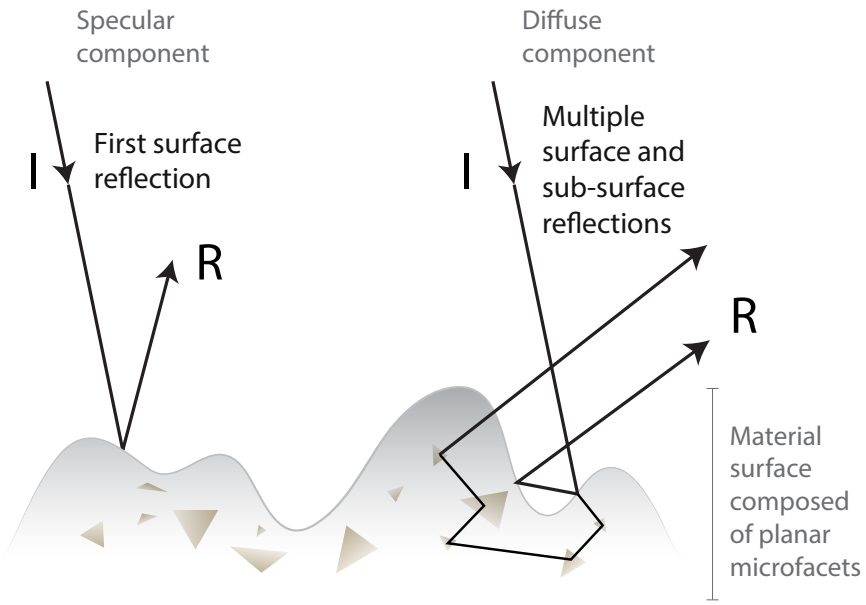

Figure 3.2: Specular and diffuse reflection from a microscopically rough material surface

The total reflected radiance f_{TS} is directly proportional to

$$f_{TS} = sf_s + df_d, \qquad s + d = 1 \tag{3.1}$$

where s and d are real non negative constants.

3.2.1 Specular Component

The specular component is given by

$$f_s = \frac{F(\theta_i, \eta)G}{\cos\theta_r} P(\alpha) \tag{3.2}$$

$F(\theta_i, \eta)$ is the Fresnel reflection coefficient, which represents the proportional attenuation of the intensity of an incident light wave with respect to specular reflection of a perfectly smooth surface. The Fresnel coefficients are defined by Eqs. 1.42.

G represents the geometric attenuation factor, which expresses the ratio of light that is not occluded by the surface due to masking or shadowing. It is a function of following form:

$$
\begin{aligned}
G &= min\left\{1, \frac{2(N\cdot H)(N\cdot V)}{(V\cdot H)}, \frac{2(N\cdot H)(N\cdot L)}{(V\cdot H)}\right\} \\
&= min\left\{1, \frac{2\cos\alpha\cos\theta_r}{\cos\theta_i'}, \frac{2\cos\alpha\cos\theta_i}{\cos\theta_i'}\right\}
\end{aligned}
\tag{3.3}
$$

$P(\alpha)$ is the probability distribution function, which predicts the distribution of the normals of the micro-facets and determines what percentage of micro-facets are oriented to reflect in the H direction. A number of different micro-facet distribution models exists. Torrance and Sparrow report a Gaussian probability distribution in the original paper from 1967 [15], thus, it is also used in this thesis.[1] The Gaussian probability distribution $P(\alpha)$ is of form

$$
P(\alpha) = \frac{1}{m^2}\cdot exp\left(-\frac{\tan^2\alpha}{m^2}\right), \tag{3.4}
$$

where m is a constant, $0 \leq m \leq 1$, which controls the apparent smoothness of the surface.

The factor $\cos\theta_r$ in the denominator of the specular component R_s determines how much of the surface is visible to the viewer.

Only those points on the surface which are aligned to specularly reflect into a given scattering direction contribute to the scatter in that direction.

3.2.2 Diffuse Component

The diffuse component is given by

$$
f_d = \cos\theta_i \tag{3.5}
$$

The diffuse component function does not require a further description as its definition is trivial.

In the following section, the Mueller matrix of the Torrance-Sparrow model is derived.

3.3 Mueller Matrix Derivation

The Torrance-Sparrow model assumes the total reflected radiance being proportional to the specular component f_s and the diffuse component f_d. Both components have to be analysed whether and how they modify the polarisation state of light.

3.3.1 Mueller Matrix of the Specular Component

The specular component is given by

$$
f_s = \frac{F(\theta_i,\eta)G}{\cos\theta_r}P(\alpha). \tag{3.6}
$$

[1] Note: Later, Cook and Torrance applied the Beckman distribution function to the Torrance-Sparrow model [16]

The geometric factor G is responsible for shadowing and masking. It defines the fraction of a facet surface that contributes to reflected radiance – obviously, it does not alter the polarisation state of the light. The probability factor $P(\alpha)$ also does not alter the polarisation state of light as it only describes the distribution of the orientation of micro-facets, and similarly the factor $\cos\theta_r$ that determines how much of the surface is visible to the viewer.

The only member of the specular component that alters the light polarisation is the Fresnel reflection coefficient $F(\theta_i, \eta)$, for which the Mueller matrix is already known (please refer to 1.7.2 and 1.7.3 for more details).

The Fresnel Mueller matrix is of form

$$\mathrm{M}_F = \begin{bmatrix} A & B & 0 & 0 \\ B & A & 0 & 0 \\ 0 & 0 & C & S \\ 0 & 0 & -S & C \end{bmatrix}, \tag{3.7}$$

with

$$\begin{aligned} A &= \frac{F_s + F_p}{2} \\ B &= \frac{F_s - F_p}{2} \\ C &= \cos(\delta_s - \delta_p) \cdot \sqrt{F_s \cdot F_p} \\ S &= \sin(\delta_s - \delta_p) \cdot \sqrt{F_s \cdot F_p} \end{aligned}. \tag{3.8}$$

After replacing the $F(\theta_i, \eta)$ by M_F, we can see that the Mueller matrix of the Torrance-Sparrow specular component, M_s, is of form

$$M_s = \frac{M_F G}{\cos\theta_r} P(\alpha) \tag{3.9}$$

3.3.2 Mueller Matrix of the Diffuse Component

The diffuse component is given by

$$f_d = \cos\theta_i. \tag{3.10}$$

Resolving the Mueller matrix for the diffuse component, M_d, is simple, as is an ideal common optical element, which serves as a depolariser. By the reason of that, M_d will be of form

$$\mathrm{M}_d = \cos\theta_i \begin{bmatrix} 1 & 0 & 0 & 0 \\ 0 & 0 & 0 & 0 \\ 0 & 0 & 0 & 0 \\ 0 & 0 & 0 & 0 \end{bmatrix}. \tag{3.11}$$

3.3.3 Mueller Matrix of the Torrance-Sparrow Model

The Mueller matrix of Torrance-Sparrow reflectance model, M_{TS}, is defined as

$$M_{TS} = s \cdot M_s + d \cdot M_d. \tag{3.12}$$

3.3.4 Verification

To verify the correctness of the statement, M_{TS} was successfully compared against the SCATMECH library.

As it was already mentioned in 2.3.3, the approach of SCATMECH library to obtain a Mueller matrix of a Torrance-Sparrow is not direct. Two sources need to be added together to simulate the Torrance-Sparrow model, namely, the shadowed facet model that simulates the specular component and a Lambertian model that simulates the diffuse component. Moreover, SCATMECH only returns Mueller matrix numerical values of the Torrance-Sparrow model obtained by converting an appropriate Jones matrix to the Mueller matrix – it does not explicitly state the Mueller matrix.

4. He-Torrance-Sillion-Greenberg Model

Another physically based reflection model allowing for polarisation was presented by X. He, K. E. Torrance, F. X. Sillion and D. P. Greenberg in 1991. [17] The model is based on wave optics and describes three types of reflection by a surface: specular, directional diffuse and uniform diffuse reflection.

The description of the He-Torrance-Sillion-Greenberg Model (HTSG) model is provided in section 4.2 and in section 4.3 the Mueller matrix for this model is stated. The HTSG Mueller matrix testing results can be found in section 6.3.

4.1 The Coordinate System

The He-Torrance-Sillion-Greenberg model uses a scalar diffraction model, so that all points on the surface contribute to the scattering in any direction. However, one needs to assume some reflectance of the surface. At that point, HTSG chooses to "vectorize" the theory by using the tangent plane approximation for determining that reflectance. For more information about the tangent plane approximation, please refer to [17], section 2.2.

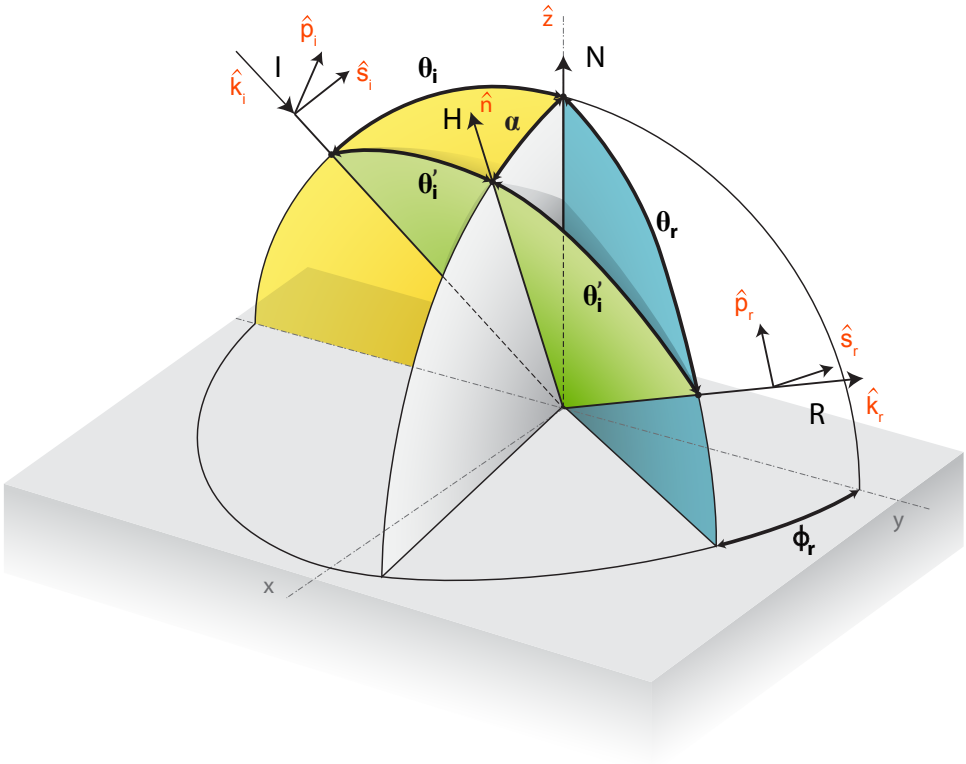

Figure 4.1: Coordinates of He-Torrance-Sillion-Greenberg model

So in other words the HTSG model uses the same angular system as is used in the Torrance-Sparrow model, however, uses its own specific vector notation to

describe it. In order to provide a backward compatibility with the original article, as well as to provide a unified overview of all glossy models investigated in this thesis, we decided to highlight the original model notation in the coordinate system by red color (see Figure 4.1).

Vectors $\hat{k}_i$, $\hat{k}_r$ denotes the wave propagation unit vectors in incident I and reflecting R direction, respectively. $\hat{s}$ and $\hat{p}$ are the polarisation unit vectors perpendicular and parallel respectively to the incident (with subscript i) and reflecting (with subscript r) direction. Term $\hat{z}$ denotes a global surface normal N and $\hat{n}$ represents local surface normal (the halfway vector H).

4.2 Overview of the Model

The He-Torrance-Sillion-Greenberg model is a diffractive model, which specify an arbitrary surface to be Gaussian distributed and spatially isotropic. Two parameters are needed to describe the surface - the root mean square (rms) roughness of the surface, σ_0, and also the autocorrelation length, τ, which is a measure of the spacing between surface peaks.

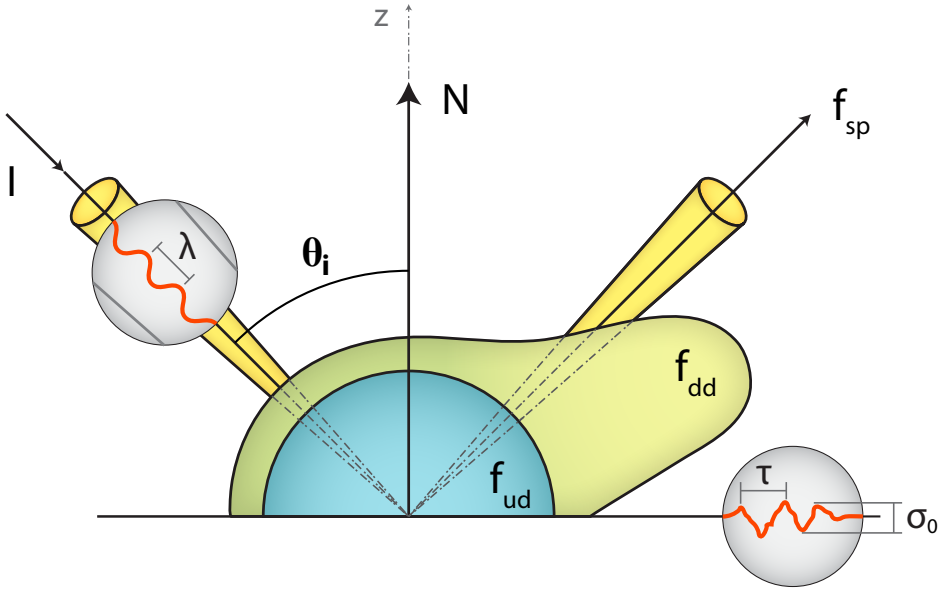

Figure 4.2: Light intensity distribution in He-Torrance-Sillion-Greenberg model

The total reflected radiance f_{HTSG} is composed of three components

$$f_{HTSG} = f_{sp} + f_{dd} + f_{ud}, \tag{4.1}$$

where the subscripts corresponds to specular (sp), directional diffuse (dd) and uniform diffuse (ud) reflection. The components f_{sp} and f_{dd} result from the first-surface reflection process, while the uniform diffuse component f_{ud} is attributed to multiple surface and/or subsurface reflections. See the Figure 4.2, which illustrates these types of reflection.

The original paper, which was published in 1991 describes mainly a physical way of deriving the model. This approach is not completely suitable for future

implementation in graphical renderer as it lacks implementation details just as at what angle the Fresnel function is evaluated and more. Hence, deep understanding of the article and some "reading between lines" is needed to find the important details that were left out and which are needed to derive the Mueller matrix.

4.2.1 Specular Component

The specular component, f_{sp}, accounts for mirror-like reflection from the mean plane of the reflecting surface. It is of form

$$f_{sp} = \frac{|F|^2 \cdot e^{-G} \cdot S}{\cos\theta_i d\omega_i} \cdot \Delta. \tag{4.2}$$

It is proportional to the Fresnel reflectivity, $|F|^2$, which is dependent on the index of refraction of the surface material, and for rough surfaces it is reduced by the surface roughness function G and the shadowing function S. Δ is a delta function which is unity in the specular cone of reflection and zero otherwise.

The geometric function G is of form:

$$G = [(2\pi\sigma/\lambda)(\cos\theta_i + \cos\theta_r)]^2 \tag{4.3}$$

where λ is a wavelength of the light and σ is the effective surface roughness, which is defined as:

$$\sigma = \frac{\sigma_0}{\sqrt{1 + \frac{z_0^2}{\sigma_0^2}}} \tag{4.4}$$

where z_0 is the root of the following equation

$$\sqrt{\frac{\pi}{2}} z = \sigma_0 K \cdot \exp\left(-\frac{z^2}{2\sigma_0^2}\right) \tag{4.5}$$

and

$$\begin{aligned} K &= K_i + K_r \\ K_i &= \frac{1}{4}\tan\theta_i \cdot erfc\left(\frac{\tau}{2\sigma_0}\cot\theta_i\right) \\ K_r &= \frac{1}{4}\tan\theta_r \cdot erfc\left(\frac{\tau}{2\sigma_0}\cot\theta_r\right) \end{aligned} \tag{4.6}$$

The shadowing function S is of form:

$$S = S_i(\theta_i) \cdot S_r(\theta_r) \tag{4.7}$$

where

$$\begin{aligned} S_i(\theta_i) &= \left(1 - \frac{1}{2}erfc\left(\frac{\tau\cot\theta_i}{2\sigma_0}\right)\right) / \left(\Lambda(\cot\theta_i) + 1\right) \\ S_r(\theta_r) &= \left(1 - \frac{1}{2}erfc\left(\frac{\tau\cot\theta_r}{2\sigma_0}\right)\right) / \left(\Lambda(\cot\theta_r) + 1\right) \end{aligned} \tag{4.8}$$

and

$$\Lambda(\cot\theta) = \frac{1}{2}\left(\frac{2}{\pi^{1/2}} \cdot \frac{\sigma_0}{\tau\cot\theta} - erfc\left(\frac{\tau\cot\theta}{2\sigma_0}\right)\right) \tag{4.9}$$

When the surface is smooth, the specular component is not attenuated by G and S since $G \to 0$ and $S \to 1$ and thus the equation 4.2 reduces to

$$\rho_{bd,sp} = \frac{|F(\theta_i', \eta)|^2}{\cos\theta_i d\omega_i} \tag{4.10}$$

4.2.2 Directional Diffuse Component

The directional diffuse reflection, f_{dd}, appears, when the wavelength of the incident light is comparable to or smaller than the projected size of surface roughness elements (i.e. $\lambda \sim \sigma\cos\theta_i$). The reflected field is diffused out to the hemisphere above the reflecting surface, but may have a directional, non uniform character. This component, comparing to the Torrance-Sparrow model, newly introduces the diffraction and interference effects. It is given by following equation

$$f_{dd} = \frac{\mathcal{F}(\hat{k}_i, \hat{k}_r, p)\cdot S}{\cos\theta_i \cdot \cos\theta_r} \cdot \frac{\tau^2}{16\pi} \cdot \sum_{m=1}^{\infty} \frac{G^m e^{-G}}{m!\cdot m} \cdot \exp\left(-\frac{\upsilon_{xy}^2\tau^2}{4m}\right). \tag{4.11}$$

$\mathcal{F}(\hat{k}_i, \hat{k}_r, p)$ is a function involving the Fresnel reflection coefficients. It is of form

$$\mathcal{F}(\hat{k}_i, \hat{k}_r, p) = \mathcal{F}(\hat{n}_b, \hat{n}_b, p)_s + \mathcal{F}(\hat{n}_b, \hat{n}_b, p)_p \tag{4.12}$$

and

$$\begin{aligned} \mathcal{F}(\hat{n}_b, \hat{n}_b, p)_s &= \delta|c_s M_{ss} + c_p M_{sp}|^2 \\ \mathcal{F}(\hat{n}_b, \hat{n}_b, p)_p &= \delta|c_s M_{ps} + c_p M_{pp}|^2 \end{aligned} \tag{4.13}$$

where

$$\begin{aligned} M_{ss} &= \left(F_s(\hat{p_i}\cdot\hat{k_r})(\hat{p_r}\cdot\hat{k_i}) + F_p(\hat{s_i}\cdot\hat{k_r})(\hat{s_r}\cdot\hat{k_i})\right) \\ M_{sp} &= -\left(F_s(\hat{s_i}\cdot\hat{k_r})(\hat{p_r}\cdot\hat{k_i}) - F_p(\hat{p_i}\cdot\hat{k_r})(\hat{s_r}\cdot\hat{k_i})\right) \\ M_{pp} &= \left(F_s(\hat{s_i}\cdot\hat{k_r})(\hat{s_r}\cdot\hat{k_i}) + F_p(\hat{p_i}\cdot\hat{k_r})(\hat{p_r}\cdot\hat{k_i})\right) \\ M_{ps} &= \left(F_s(\hat{p_i}\cdot\hat{k_r})(\hat{s_r}\cdot\hat{k_i}) - F_p(\hat{s_i}\cdot\hat{k_r})(\hat{p_r}\cdot\hat{k_i})\right) \end{aligned} \tag{4.14}$$

and

$$\delta = \left(\frac{2\pi}{\lambda}\right)^2 \cdot \frac{|\hat{k_r} - \hat{k_i}|^4}{|\hat{k_r}\times\hat{k_i}|^4\left(\hat{z}\cdot(\hat{k_r} - \hat{k_i})\right)^2}. \tag{4.15}$$

Terms c_s and c_p are called the polarisation coefficients on the incident light fields. They belongs to an interval $(0, 1)$, where $c_s + c_p = 1$. Terms $\hat{k}_i$ are $\hat{k}_r$ are unit vectors in incident and reflection direction, respectively.

Terms F_s and F_p are the Fresnel reflection coefficients, which are evaluated at the bisecting angle ψ given by $\psi = \cos^{-1}(|\hat{k}_r - \hat{k}_i|/2)$, $\hat{z}$ is a unit global surface normal and $\hat{s_i}$, $\hat{p_i}$, $\hat{s_r}$, $\hat{p_r}$ are unit polarisation vectors. They are given by

$$\begin{aligned} \hat{s}_i &= \frac{\hat{k}_i \times \hat{z}}{|\hat{k}_i \times \hat{z}|} \\ \hat{p}_i &= \hat{s}_i \times \hat{k}_i \\ \hat{s}_r &= \frac{\hat{k}_r \times \hat{z}}{|\hat{k}_r \times \hat{z}|} \\ \hat{p}_r &= \hat{s}_r \times \hat{k}_r \end{aligned} \tag{4.16}$$

where $\times$ denotes the cross product of two vectors.

Letter p denotes the polarisation state vector of the incident light, which is defined as

$$p = c_s \hat{s}_i + c_p \hat{p}_i \tag{4.17}$$

Term v_{xy} is a function which depends on the illumination and reflection angles and it is defined as

$$\begin{aligned} v_{xy} &= \sqrt{v_x^2 + v_y^2} \\ v &= \frac{2\pi}{\lambda}(\hat{k}_r - \hat{k}_i) \end{aligned} . \tag{4.18}$$

It can be seen that when the surface is smooth and the specular component dominates the first-surface reflection process, the contribution from the directional diffuse component diminishes to zero.

The reflected intensity depends on the surface roughness σ and the autocorrelation length τ.

4.2.3 Uniform Diffuse Component

The uniform diffuse component, f_{ud}, represents the light reflected by multiple surface reflections or by subsurface reflections. The analytical results suggest that the reflected field may be approximated as nearly directionally uniform, therefore the multiply-reflected and/or subsurface scattered light is taken for Lambertian diffuse. The uniform diffuse component may be expressed as

$$f_{ud} = a(\lambda). \tag{4.19}$$

4.3 Mueller Matrix Derivation

The overview about the HTSG model shows that there are two terms, which are described to be somehow related to the Fresnel reflection coefficients, namely, $|F|^2$ (from the specular component) and $\mathcal{F}(\hat{k}_i, \hat{k}_r, p)$ (from the directional diffuse component). The original article is incomplete regarding to an exact definition of these terms and relationships between them, it only says that "$|F|^2$ *is the Fresnel reflectivity which depends on the index of refraction*" and "$\mathcal{F}$ *is a function*

involving Fresnel reflection coefficients" [17], referring the reader to Eqs. (68), (59) and (60) from the original paper. [1] Investigating the Eq. (68), we also found another Fresnel related terms, the Fresnel reflection coefficients F_s and F_p, which should be evaluated at the bisecting angle given by $\cos^{-1}(|\hat{k}_r - \hat{k}_i|/2)$.

Clarification of the relationships between $|F|^2$, $\mathcal{F}(\hat{k}_i, \hat{k}_r, p)$, F_s and F_p is essential for Mueller matrix derivation.

The definition of the F_s and F_p terms is already done in the original paper. These expressions denote the Fresnel reflection coefficients, the same as are described in chapter 1.7.2.

The expression $\mathcal{F}(\hat{k}_i, \hat{k}_r, p)$ from Eq. 4.12 reads

$$\begin{aligned} F_s &= \delta|c_s M_{ss} + c_p M_{sp}|^2 \\ F_p &= \delta|c_s M_{ps} + c_p M_{pp}|^2 \end{aligned} \tag{4.20}$$

We can write this as

$$\begin{aligned} F_s &= \delta|d_s|^2 \\ F_p &= \delta|d_p|^2 \end{aligned} \tag{4.21}$$

where

$$\begin{pmatrix} d_s \\ d_p \end{pmatrix} = \begin{pmatrix} M_{ss} & M_{sp} \\ M_{ps} & M_{pp} \end{pmatrix} \cdot \begin{pmatrix} c_s \\ c_p \end{pmatrix}. \tag{4.22}$$

It is then apparent that this is a Jones relationship, where

$$\begin{pmatrix} c_s \\ c_p \end{pmatrix} \tag{4.23}$$

is an incident Jones vector,

$$\begin{pmatrix} M_{ss} & M_{sp} \\ M_{ps} & M_{pp} \end{pmatrix} \tag{4.24}$$

is a Jones matrix, and

$$\begin{pmatrix} d_s \\ d_p \end{pmatrix} \tag{4.25}$$

is the output Jones vector. The total intensity associated with the output Jones vector is

$$|d_s|^2 + |d_p|^2 \tag{4.26}$$

Since the authors of the HTSG model were not interested in the Stokes vector for the scattered light, and were only interested in the intensity (its first element), they simply left this expression as is. There are, however, Stokes vector equivalents of Eqs. 4.23 and 4.25. The relationship between them is the Mueller matrix derived from Eq. 4.24 using Eqs. 1.36 and 1.37.

Goldstein prove this in [3]. Fore the sake of completeness, we briefly discuss it. The i-th element of the Stokes vector of Eq. 4.23 is

[1] In the context of this thesis, the Eq. (68) corresponds to Eq. 4.12 and Eqs. (59) and (60) to Eq. 4.13.

$$c^\dagger \sigma_i c \tag{4.27}$$

where $c = (c_s, c_p)^T$. Thus,

$$d^\dagger \sigma_j d = c^\dagger M^\dagger \sigma_j M c = \frac{1}{2} \sum_i c^\dagger M^\dagger \sigma_j M \sigma_i \sigma_i c \tag{4.28}$$

This can be written as

$$\frac{1}{2} \sum_i c^\dagger M^\dagger \sigma_j M \sigma_i \sigma_i c = \sum_i \frac{1}{2} Tr(M^\dagger \sigma_j M \sigma_i)(c^\dagger \sigma_i c), \tag{4.29}$$

from which it can be seen that the Mueller matrix of M is

$$\frac{1}{2} Tr(M^\dagger \sigma_j M \sigma_i). \tag{4.30}$$

where Tr is a trace of a matrix, $M^\dagger$ is the Hermitian conjugate of M and σ_i denotes the Pauli matrices. This is an important observation. Besides, the absolute value of the square of a Jones matrix is the Mueller matrix derived from it, which comes from the definition of the Stokes vector. [3].

Finally, the $|F|^2$ term serves to determine the reflectance on a specular surface. This description together with the absolute value and a magnitude-square multiplication suggest that $|F|^2$ stands for a Jones matrix of a Fresnel, J_F, which is of form

$$F = J_F = \left| \begin{pmatrix} F_s & 0 \\ 0 & F_p \end{pmatrix} \right|^2 \tag{4.31}$$

4.3.1 Mueller Matrix of the Specular Component

The specular component, f_{sp}, is of form

$$f_{sp} = \frac{|F|^2 \cdot exp(-G) \cdot S}{\cos\theta_i d\omega_i} \cdot \Delta. \tag{4.32}$$

Terms G and S are functions that are responsible for shadowing and masking and also for attenuating of the specular term, but none of them are a function of polarisation. That can also be seen from Eqs. 4.3– 4.9, which involve only angles and constants computation. The Δ function takes only constant values 0 and 1. The term $d\omega_i$ represents the differential solid angle, which is important for the derivations, but is ignored for practical purposes.

The only polarising member of the specular component is $|F|^2$, which is equal to a magnitude-square multiplication of J_F in absolute value, i.e.

$$F = J_F = \left| \begin{pmatrix} F_s & 0 \\ 0 & F_p \end{pmatrix} \right|^2. \tag{4.33}$$

An equivalent to this formula in terms of the Mueller matrix calculus is the Fresnel Mueller matrix, M_F, which is of form

$$\mathrm{M}_F = \begin{bmatrix} A & B & 0 & 0 \\ B & A & 0 & 0 \\ 0 & 0 & C & S \\ 0 & 0 & -S & C \end{bmatrix}, \tag{4.34}$$

with

$$\begin{aligned} A &= \frac{F_s + F_p}{2} \\ B &= \frac{F_s - F_p}{2} \\ C &= \cos(\delta_s - \delta_p) \cdot \sqrt{F_s \cdot F_p} \\ S &= \sin(\delta_s - \delta_p) \cdot \sqrt{F_s \cdot F_p} \end{aligned} \tag{4.35}$$

The Mueller matrix of the specular component, M_{sp} is then of form

$$M_{sp} = \frac{M_F \cdot exp(-G) \cdot S}{\cos\theta_i d\omega_i} \cdot \Delta. \tag{4.36}$$

4.3.2 Mueller Matrix of the Directional Diffuse Component

The directional diffuse component, f_{dd}, becomes more significant with increasing roughness of the surface. It is defined as

$$f_{dd} = \frac{\mathcal{F}(\hat{k}_i, \hat{k}_r, p) \cdot S}{\cos\theta_i \cdot \cos\theta_r} \cdot \frac{\tau^2}{16\pi} \cdot \sum_{m=1}^{\infty} \frac{G^m exp(-G)}{m! \cdot m} \cdot \exp\left(-\frac{\upsilon_{xy}^2 \tau^2}{4m}\right). \tag{4.37}$$

Out of all members in this equation, the $\mathcal{F}(\hat{k}_i, \hat{k}_r, p)$ term is the only member affecting the polarisation state of light – all the other members are scalars and does not affect polarisation.

In the introduction to the section 4.3 we have observed that $\mathcal{F}(\hat{k}_i, \hat{k}_r, p)$ contains a Jones matrix which, after substituting Eqs. 4.14, results in a complicated Jones matrix, which stands for the Fresnel Jones matrix, $J_{F_{s-p}}$,

$$J_{F_{s-p}} = \begin{pmatrix} (F_s(\hat{p_i} \cdot \hat{k_r})(\hat{p_r} \cdot \hat{k_i}) + F_p(\hat{s_i} \cdot \hat{k_r})(\hat{s_r} \cdot \hat{k_i}) & -\left(F_s(\hat{s_i} \cdot \hat{k_r})(\hat{p_r} \cdot \hat{k_i}) - F_p(\hat{p_i} \cdot \hat{k_r})(\hat{s_r} \cdot \hat{k_i})\right) \\ (F_s(\hat{p_i} \cdot \hat{k_r})(\hat{s_r} \cdot \hat{k_i}) - F_p(\hat{s_i} \cdot \hat{k_r})(\hat{p_r} \cdot \hat{k_i}) & (F_s(\hat{s_i} \cdot \hat{k_r})(\hat{s_r} \cdot \hat{k_i}) + F_p(\hat{p_i} \cdot \hat{k_r})(\hat{p_r} \cdot \hat{k_i}) \end{pmatrix} \tag{4.38}$$

reporting in the s-p basis. By reason of that, $J_{F_{s-p}}$ has to perform a rotation into the scattering basis. This rotation is not symmetric, because the s-p basis for the incident light is rotated by a different angle than the s-p basis for the outgoing light, hence,

$$J'_F = R_1 J_{F_{s-p}} R_2 \tag{4.39}$$

where J'_F denotes a Fresnel Jones matrix obtained by rotation and R_1 and R_2 are two different rotation matrices. This approach is defined in the original article, however, we have successfully derived a simpler version of a Jones matrix, which

corresponds to J'_F, but is more intuitive easier to read. The matrix already refers to the scattering plane and is denoted by J_{dd} For more details about the derivation, please refer to Attachment A.

The simpler version J_{dd} is of form

$$J_{dd} = \begin{pmatrix} F_s & 0 \\ 0 & F_p \end{pmatrix} \cdot (k_i \times k_r)^2. \tag{4.40}$$

The Mueller matrix of J_{dd} will be obtained by converting J_{dd} into a corresponding Mueller matrix, M'_{dd}, using Eqs. 1.36 and 1.37 mentioned in section 1.6.

Having M'_{dd} stated, determining the Mueller matrix of the directional diffuse component, M_{dd}, is simple:

$$M_{dd} = \frac{\delta \cdot M'_{dd} \cdot S}{\cos\theta_i \cdot \cos\theta_r} \cdot \frac{\tau^2}{16\pi} \cdot \sum_{m=1}^{\infty} \frac{G^m exp(-G)}{m! \cdot m} \cdot \exp\left(-\frac{\upsilon_{xy}^2 \tau^2}{4m}\right) \tag{4.41}$$

4.3.3 Mueller Matrix of the Uniform Diffuse Component

The derivation of the Mueller Matrix of the uniform diffuse component, M_{ud}, which is of form

$$f_{ud} = a(\lambda) \tag{4.42}$$

is trivial, as the multiply-reflected and/or subsurface scattered light is approximated as Lambertian diffuse, which serves as a depolariser. Therefore, M_{ud} will be of form

$$\mathrm{M}_{ud} = a(\lambda) \begin{bmatrix} 1 & 0 & 0 & 0 \\ 0 & 0 & 0 & 0 \\ 0 & 0 & 0 & 0 \\ 0 & 0 & 0 & 0 \end{bmatrix}. \tag{4.43}$$

4.3.4 Mueller Matrix of the He-Torrance-Sillion-Greenberg Model

The Mueller matrix of He-Torrance-Sillion-Greenberd reflectance model, M_{HTSG}, is defined as

$$M_{HTSG} = M_{sp} + M_{dd} + M_{ud}. \tag{4.44}$$

5. Weidlich-Wilkie Model

Many natural materials are composed of multiple layers (i.e. plastics, varnished metals, etc.), which exhibits a typical appearance, which is hardly simulated by simpler BRDF models. In 2007, a layered surface reflection model was introduced by A. Weidlich and A. Wilkie [19]. The model presents a method combining several micro-facet based surface layers into a single unified one allowing us to achieve new visual visual phenomenon. The model can simulate both smooth and rough multi-layered surfaces and includes absorption within the layers, as well as total internal reflection.

The basic concept overview of the model is provided in section 5.2 and the Mueller matrix for this model is derived in the section 5.3 Mueller matrix testing results can be found in section 6.4.

5.1 The Coordinate System

Even thought it is not mentioned explicitly in the original paper, the coordinate system used by the Weidlich-Wilkie model for each layer is the same as the one used in Torrance-Sparrow model. Further description of the coordinate system can be found in the section 1.3.

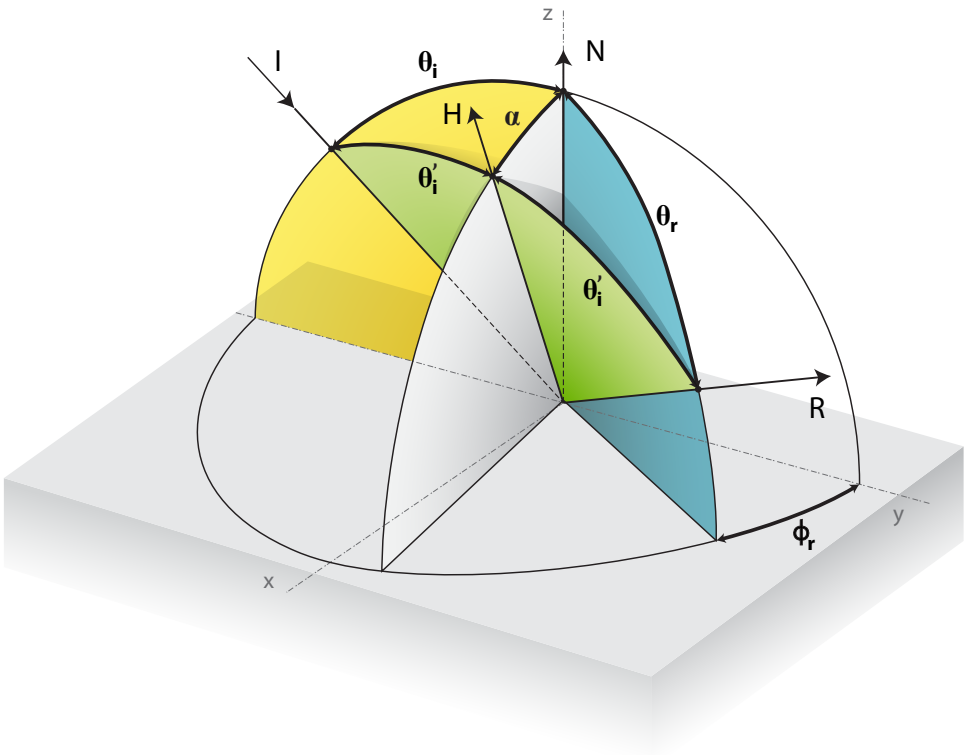

Figure 5.1: Spatial angles of incident and reflected radiance

5.2 Overview of the Model

The basic idea of the Weidlich-Wilkie model is that the surface material is composed of thin layers, which can have any arbitrary BRDF (i.e. perfect mirror, Lambertian surface, Torrance-Sparrow, ...), for which a transmission component exists (except for the lowest layer). The individual layered components together give rise to a more sophisticated BRDF. However, using such model in a renderer in an unrestricted version would involve unwanted sub-surface scattering computations within the layers, that make the model evaluation very slow or even unusable. Therefore, the classical assumption and simplifications are proposed:

- The thickness of a layer is small enough, i.e. any micro-facet is much larger in horizontal extent in relation to the layer thickness, which allows us to neglect the distance between the directly reflected ray and the ray resulting from propagation through the layer. We can then assume the following (see Figure 5.2):
  - a ray will always leave through the same micro-facet that it entered through,
  - any exiting ray coming from a lower level will emanate from the original point of entry. This point is highlighted in yellow color. The direction of these rays is computed according to the correct geometry (dashed line).
- All rays that refract on the surface are assumed to meet at a single point on the next layer interface.
- All light scattering is due to reflection at the boundaries between layers; no scattering occurs within individual layers.
- The material used for any (partially) transparent layers only attenuates light passing through, and does not contribute any secondary scattering effects of its own.

Due to the simplifications, the model is limited to surfaces that have layers thick enough to have the influence of absorption, and sufficiently thin enough that the model's simplification holds true.

The evaluation of the entire Weildich-Wilkie BRDF model for arbitrary input and output direction is carried out in a recursive manner as follows (see Figure 5.3):

1. Any incoming light that encounters an interface between the first and second layer in the layer stack, is partly reflected from and partly transmitted into the second layer. The BRDF of the topmost layer, f_{W_1}, is evaluated for the two given incoming and outgoing directions, ω_i and ω_o. This yields a reflection component, and, except for the lowest layer, two refraction directions. The actual amount of energy to be refracted is determined by the Fresnel transmittance coefficient $T_{12} = 1 - F_{12}$ (F_{12} denotes a Fresnel function) and the refracted light follows the two refraction directions associated with the initial incident directions.

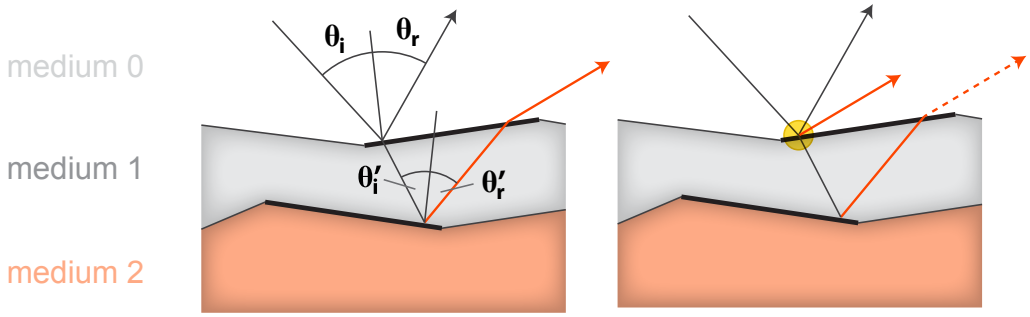

Figure 5.2: This diagram describes the light intensity distribution defined by Weidlich-Wilkie model. When a light wave strikes an interface between two different media, some of the energy is reflected from that interface, propagates in the mirror direction and stays within the first medium. Often a part of the energy enters the second media as well and continue its propagation there. The relationship between the angle of incidence, θ_i, and angle of refraction, θ_r, is given by the Snell's Law. Diagram courtesy [19].

2. The T_{12} amount of the light enters the second layer. A part of this is possibly absorbed by the absorption term, a, and the rest then interacts with the surface of the second layer, f_{W_2}, - the process is recursively started at step 1 until an opaque layer without a transmission component defined is encountered.

3. All light that is reflected from lower layers is again attenuated by the T_{21} on its upward path on the return from recursion, and possibly subjected to total internal reflection, t. The contributions from both layers are added together.

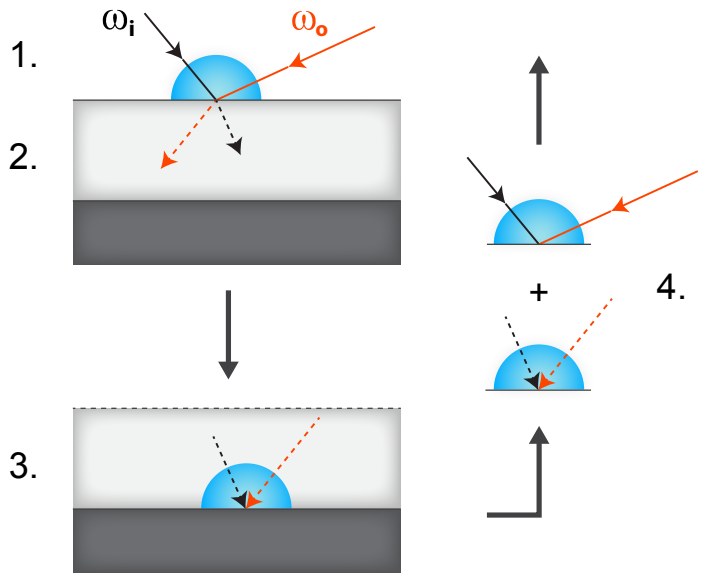

Figure 5.3: This diagram shows the recursive BRDF evaluation process. Diagram courtesy [19].

Mathematically this can be expressed as:

$$f_{WW} = f_{W_1}(\theta_i, \theta_r) + T_{12} \cdot f_{W_2}(\theta_i', \theta_r') \cdot a \cdot t \tag{5.1}$$

where a is the attenuation term according to Bourguer-Lambert-Beer law. The portion of absorbed light depends on the material-specific wavelength-dependent absorption coefficient, α, and the distance the light travels in a particular layer. The attenuation term a is of form [20]

$$a = \exp\left(-\alpha d \cdot \left(\frac{1}{\theta_{i'}} + \frac{1}{\theta_{r'}}\right)\right) \tag{5.2}$$

where d is the thickness of the layer. The t_i term denotes the internal reflection term, which compensates for the energy lost during the potential total internal reflection of light, when crossing an inter layer boundary from denser into a less dense medium on its way upwards. [20] It is of following form

$$t = (1 - G) + T_{21} \cdot G \tag{5.3}$$

where G is the Torrance-Sparrow geometry attenuation term. For more details, please refer to 3.3.

5.3 Mueller Matrix Derivation

The Weidlich-Wilkie model is a recursive model. In one step of recursion, the model considers behaviour of two neighbouring layers. To increase the readability, we will divide the main formula defining the model into two parts – the first and the second layer.

5.3.1 Mueller Matrix of the First layer

The interaction of the light with the first layer, f_{W_1}, in the layer stack is defined as

$$f_{W_1}(\theta_i, \theta_r). \tag{5.4}$$

The term $f_{W_1}(\theta_i, \theta_r)$ determines how much of the light energy is reflected, respectively refracted to the next layer. This behaviour can be expressed by the Fresnel reflection coefficients. Hence, the Mueller matrix of the first surface, M_{W_1}, is obtained by replacing $f_{W_1}(\theta_i, \theta_r)$ by M_F. M_{W_1} is then of form

$$\mathrm{M}_{W_1} = M_F = \begin{bmatrix} A & B & 0 & 0 \\ B & A & 0 & 0 \\ 0 & 0 & C & S \\ 0 & 0 & -S & C \end{bmatrix}, \tag{5.5}$$

with

$$\begin{aligned} A &= \frac{F_s + F_p}{2} \\ B &= \frac{F_s - F_p}{2} \\ C &= \cos(\delta_s - \delta_p) \cdot \sqrt{F_s \cdot F_p} \\ S &= \sin(\delta_s - \delta_p) \cdot \sqrt{F_s \cdot F_p} \end{aligned} . \tag{5.6}$$

5.3.2 Mueller Matrix of the Second Layer

The second layer is defined as

$$T_{12} \cdot f_{W_2}(\theta_i', \theta_r') \cdot a \cdot t. \tag{5.7}$$

The term T_{12}, respectively T_{21}, which is contained in t, describes the remaining portion of the incident light that goes to the second level, respectively back to the first level of surfaces. It is attenuated by factors a and t, but does not change the state of polarisation. The term $f_{W_2}(\theta_i', \theta_r')$ determines the amount of energy that would be reflected and refracted, which can be accomplished by the Fresnel reflection coefficients. It can be seen that the only polarising term is $f_{W_2}(\theta_{i'}, \theta_{r'})$. The term $f_{W_2}(\theta_{i'}, \theta_{r'})$ denotes the BRDF of the second layer. By reason of that, it will be replaced by a corresponding Mueller matrix. In the original paper, there were three types of the second surface mentioned - Torrance-Sparrow, Oren-Nayar and Lambert. Lambertian Mueller Matrix is a perfect depolariser and its Mueller matrix is defined in Eq. 1.26. The Mueller matrix of the Torrance-Sparrow model is derived in chapter 3.

Thus, the Mueller matrix of the second layer of the Weidlich-Wilkie model, M_{W_2} is of following form:

$$M_{W_2} = T_{12} \cdot M_{surface} \cdot a \cdot t \tag{5.8}$$

where $M_{surface}$ denotes a Mueller matrix of the second surface.

5.3.3 Mueller Matrix of the Weidlich-Wilkie Model

The Mueller matrix of the Weidlich-Wilkie model M_{WW} is then defined as

$$\mathrm{M}_{WW} = M_{W_1} + M_{W_2} = M_{W_1} + T_{12} \cdot M_{surface} \cdot a \cdot t. \tag{5.9}$$

6. Results

The Mueller matrices derived in chapters 3, 4 and 5 were incorporated in ART, a polarisation capable renderer. *Note: The implementation of the Mueller matrices in ART is not a subject of this master thesis and the author of this master thesis is not the author of the implementation.*

As a testing scene, we used a simple scene containing a sphere covered with a polarising version of each glossy BRDF, standing on a perfectly smooth black glass floor. We used a diffuse light to illuminate the scene.

The scene itself, the overall degree of polarisation, the degree of linear horizontal or vertical polarisation, the degree of linear polarisation rotated by 45° and the degree of right or left circular polarisation was visualized for each of the BRDFs. ART uses specified colours for this visualization.

The abbreviations used to describe the images and the colours that visualize the intensity of polarisation are following

- Degree of polarisation (red)
- SC1 – shows 0°/90° linear polarisation (red, green)
- SC2 – shows 45°/135° linear polarisation (red, green)
- SC3 – shows right/left circular polarisation (red, green)

6.1 The Fresnel Model

For the sake of the completeness, a sphere with a perfectly specular, Fresnel, surface was also rendered and visualized in terms of polarisation. The sphere, that we can see on the left in Figure 6.1 shows a golden, perfectly smooth sphere. Due to the fact that the sphere is a conductor, we can see that the the overall degree of polarisation is not as strong as it is on the dielectric floor. That is an expected behaviour, please, refer to the Figure 1.13 for conductors and the Figure 1.7 for dielectrics behaviour graph.

6.2 The Torrance-Sparrow Model

The scene in Figure 6.3 shows a glossy conductive golden sphere with Torrance-Sparrow surface. The diffuse component is not very strong, hence, the overall degree of polarisation is pretty strong. The stronger the diffuse component is, the darker the sphere would appear in the degree-of-polarisation image.

6.3 He-Torrance-Sillion-Greenberg

The sphere with the metallic HTSG surface on the Figure 6.5 is defined by the surface parameters $\sigma_0 = 20$ micrometers and $\tau = 0.20$ micrometers. The surface is more diffuse than the one observed in the case of the Torrance-Sparrow model, which causes decreasing of the overall polarisation on the sphere (the sphere appears darker).

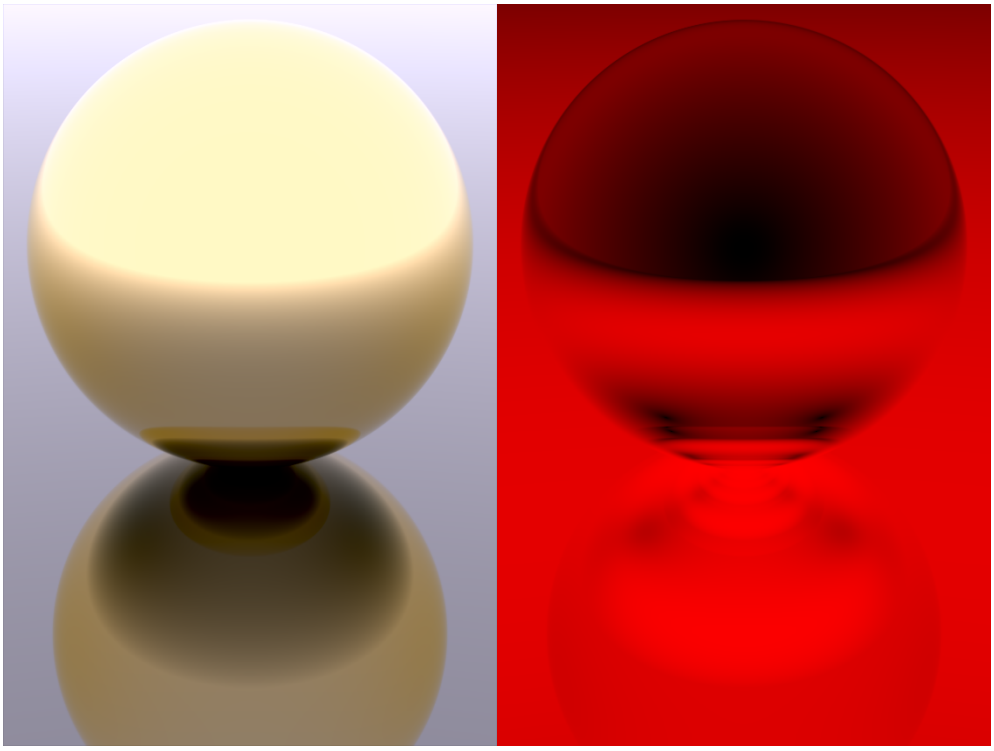

Figure 6.1: Fresnel. **Left:** A simple scene showing a conductive, perfectly specular sphere. **Right:** Degree of Polarisation

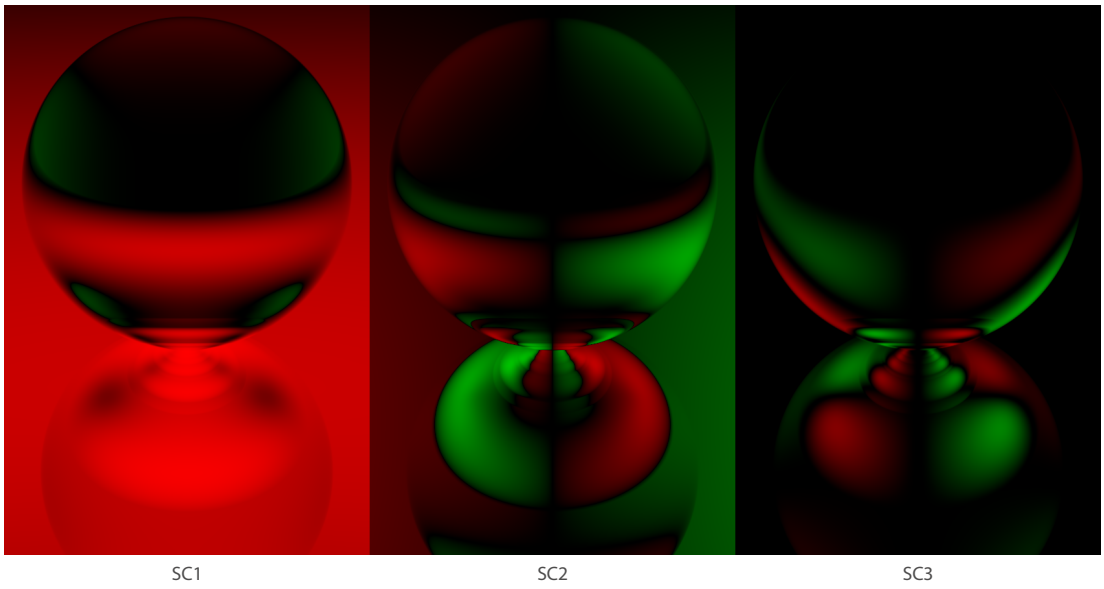

Figure 6.2: The direct visualisations of the three Stokes vector components, i.e. S_1, S_2, S_3, for the Fresnel model.

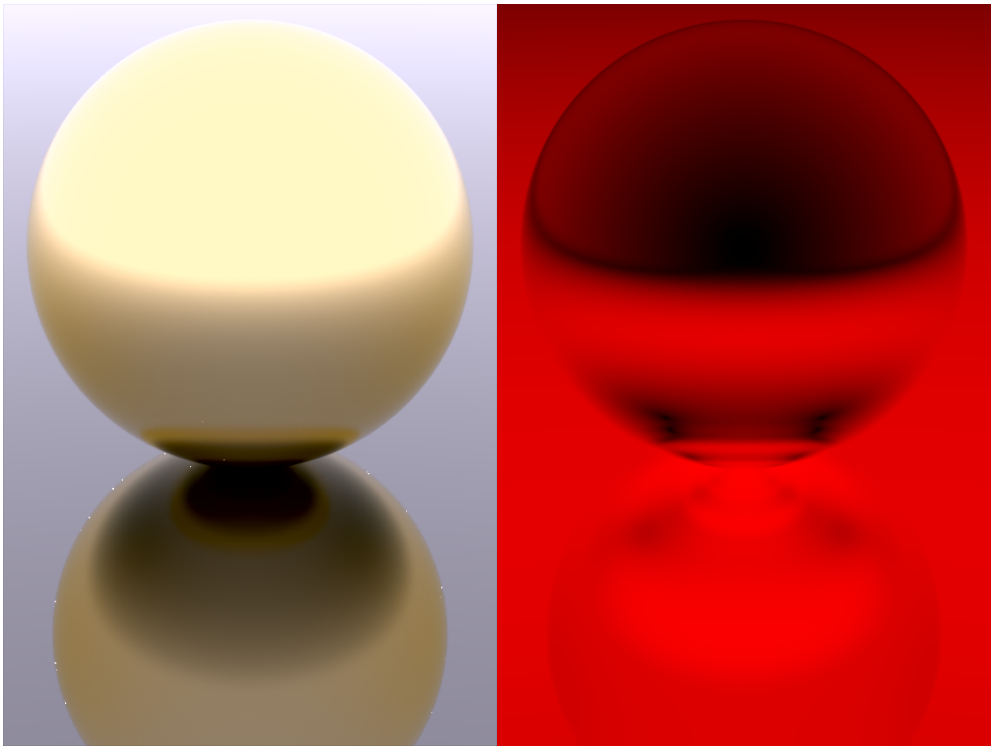

Figure 6.3: The Torrance-Sparrow model. **Left:** A simple scene showing a sphere with a golden Torrance-Sparrow BRDF surface. **Right:** Degree of Polarisation

Figure 6.4: The direct visualisations of the three Stokes vector components, i.e. S_1, S_2, S_3, for the Torrance-Sparrow model.

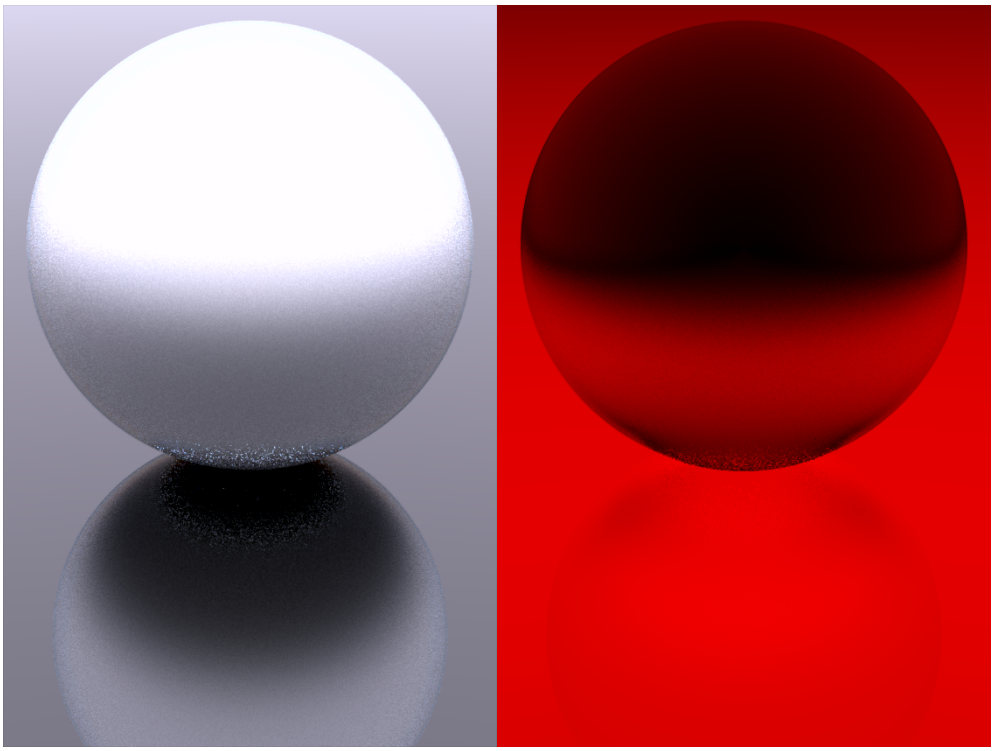

Figure 6.5: The He-Torrance-Sillion-Greenberg model. **Left:** A simple scene showing an alluminium sphere with HTSG BRDF surface. **Right:** Degree of Polarisation

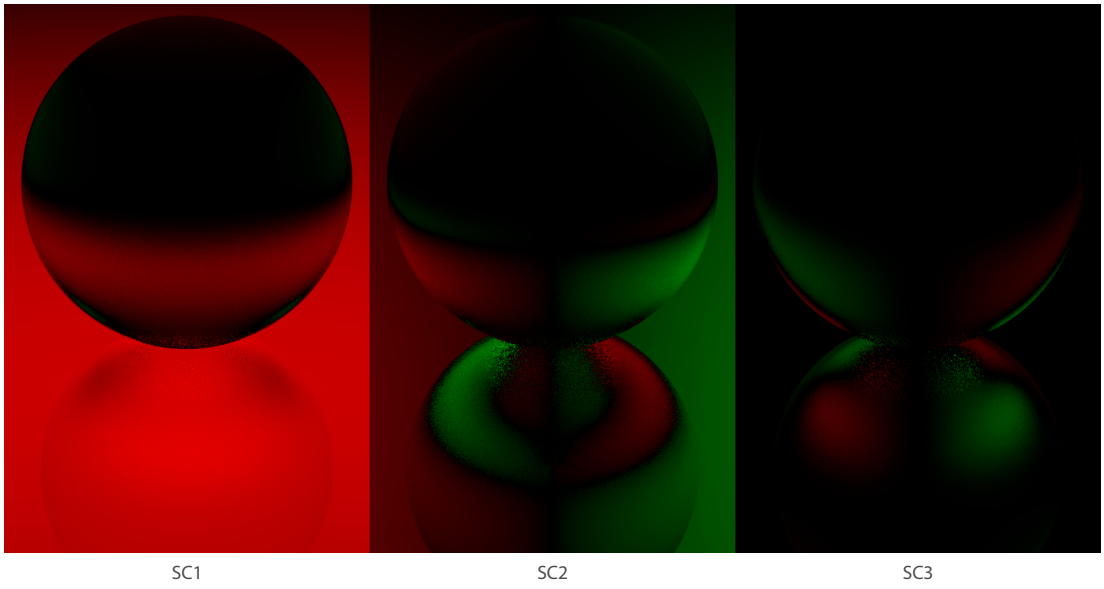

Figure 6.6: The direct visualisations of the three Stokes vector components, i.e. S_1, S_2, S_3, for the He-Torrance-Sillion-Greenberg model.

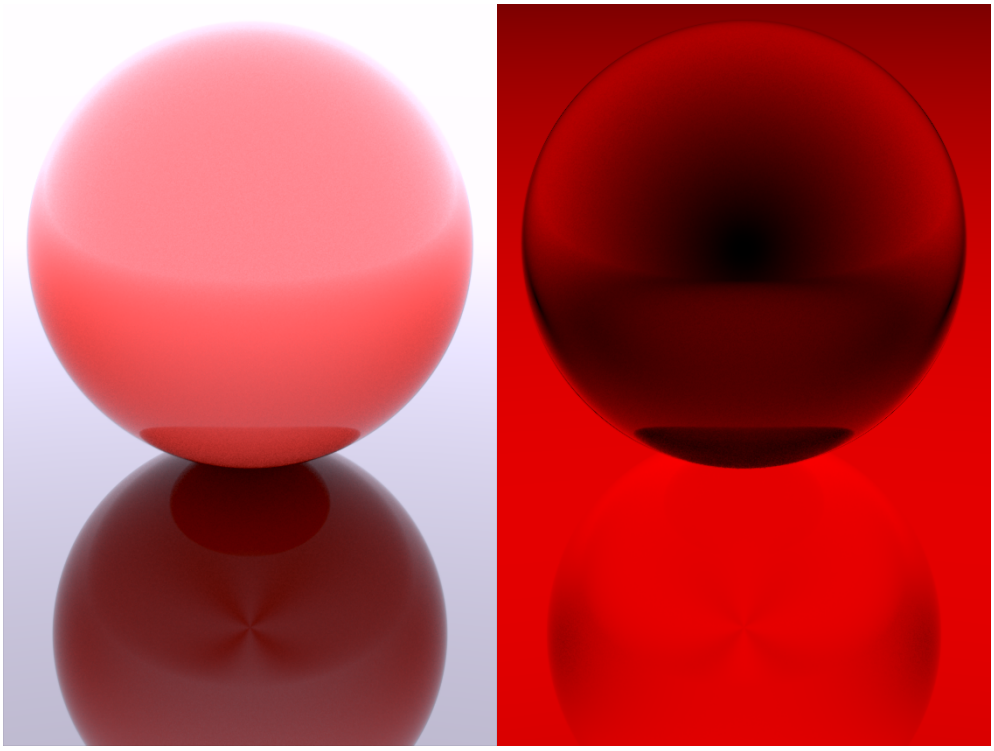

Figure 6.7: The Weidlich-Wilkie model. **Left:** A simple scene showing a sphere with the Weidlich-Wilkie BRDF surface. **Right:** Degree of Polarisation

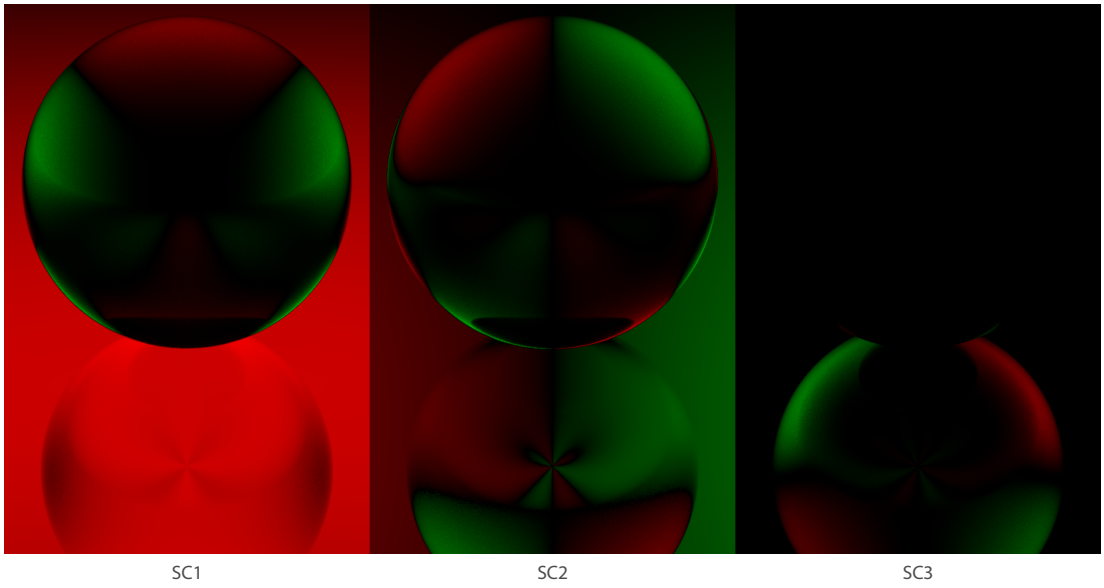

Figure 6.8: The direct visualisations of the three Stokes vector components, i.e. S_1, S_2, S_3, for the Weidlich-Wilkie model.

6.4 Weidlich-Wilkie

The layered Weidlich-Wilkie model sphere was rendered using the following parameters – the upper coat is made of glass and the subsurface is given by a red Lambert BRDF. The Figure 6.7 shows the combination effect of clearcoat top and diffuse layer underneath.

Conclusion

In this thesis, we have derived polarising versions of realistic glossy BRDF models, namely, Torrance Sparrow, He-Torrance-Sillion-Greenberg and Weidlich-Wilkie BRDF models. The process of acquiring the polarising versions of these models included a systematic Mueller matrix derivation for each of them, as Mueller Matrix is a mathematical construct used to describe the state of polarisation that the light can be subjected to, when it interacts with a polarising medium. Each model underwent an analysis, in which factors affecting polarisation had been found and expressed in form of Mueller matrices.

The Fresnel lighting model played the key role by reason of having the Mueller matrix already stated. All examined models assume a micro-facet surface, i.e. surface consisting of small, randomly disposed, perfectly specular planar facets. These facets reflect light in a mirror-like fashion, refracting certain amount of light energy under the surface (or no energy in case of Brewster's angle) and this behaviour is exactly what can be described by Fresnel. Moreover, Fresnel reflection coefficients don't just state the amount of incident light intensity that is reflected for the perpendicular and parallel components of the reflected light, but also describe the phase-shift, whose inclusion is essential to simulate phenomena of conversion of linearly polarized light into elliptically polarized.

The final rendered images are in close agreement with the expected results. Derived Mueller matrices were tested with various input parameters using Wolfram Mathematica. These simulations as well as the rendered images show promising results and support the validity of the proposed solution. In the future research, number of rendered scenes should be extended and the implementation in the ART system improved. Further investigation and verification of the derived Mueller matrices using wider data set can be another research task.

Due to the fact that these polarising glossy BRDF models are suitable for computer graphics purposes, we have significantly contributed to the realistic rendering field and, thus, highlighted a number of topics on which further research would be beneficial. Better visual results can be obtained in reference simulations, where highly accurate renderings might not be used for production shots, but where it serves to make sure a non-polarising renderer is not making any mistakes by omitting polarisation. Also preview of how certain scenes (car cockpits) look when one is wearing anti-glare sunglasses (i.e. polarising sunglasses) can be achieved, which is important for car industry. Reference code for brute force offline simulations can also favour from this thesis results. Reference scattering computations for complex materials, e.g. complicated sub-surface geometries can now be achieved.

Bibliography

[1] Savenkov, Sergey N. *Jones and Mueller matrices: structure, symmetry relations and information content*. Springer Berlin Heidelberg, 2009. ISBN: 978-3-540-74276-0.

[2] Wilkie, Alexander, Weidlich, Andrea. *SIGGRAPH Asia 2012 Course Notes Polarised Light in Computer Graphics Parts 1 & 2*. September 2012.

[3] Goldstein, Dennis. *Polarized Light*. Second Edition, Revised and Expanded. Marcel Dekker Inc., New York, USA, 2003. ISBN: 0-8247-4053-X.

[4] Ghost, Abhijeet, Hawkins, Tim, Peers, Pieter, Frederiksen, Sune, Debevec, Paul E. *Practical modeling and acquisition of layered facial reflectance*. ACM Trans. Graph, 27(5):139, 2008.

[5] Meseth, Jan, Hempel, Shawn, Weidlich, Andrea, Fyffe, Lynn, Fyffe, Graham, Miller, Craig, Carroll, Paul, Debevec, Paul E. *Improved linear light source material reflectance scanning*. ACM SIGGRAPH 2012 Talks, SIGGRAPH '12, pages 11:1–11:1, New York, NY, USA, 2012. ACM.

[6] Collett, Edward. *Field Guide to Polarization*. SPIE PRESS, Bellingham, Washington, USA, 2005. ISBN: 0-8194-5868-6.

[7] Wilkie, Alexander, Weidlich, Andrea, Zotti, Georg. *ART for Newbies, The Advanced Rendering Toolkit Installation and User Manual*. Version: 2.0.0-Alpha-028

[8] *CodeItNow*. http://www.rorydriscoll.com/2008/08/24/lighting-the-rendering-equation/. 16. 5. 2013, 2:48

[9] Kajiya, James T. *The Rendering Equation*. Siggraph 1986: 143, doi:10.1145/15922.15902, ISBN 0-89791-196-2

[10] Hanka, Adam, Kahoun, Martin. *Přednáška 2: Světlo, radiometrie*. Počítačová grafika III (NPGR010), 15. října 2012.

[11] Bártová, Kristina. *Přednáška 3: Odraz světla, BRDF*. Počítačová grafika III (NPGR010), 4. října 2012.

[12] Dominec, Adam, Navrátil, Jan. *Přednáška 4: Zobrazovací rovnice*. Počítačová grafika III (NPGR010), 27. října 2012.

[13] Vévoda, Petr. *Přednáška 7: Path Tracing II*. Počítačová grafika III (NPGR010), 15. listopadu 2012.

[14] Křivánek, Jaroslav. *Počítačová grafika III – Odraz světla, BRDF*. http://cgg.mff.cuni.cz/ jaroslav/teaching/2012-NPGR010/slides/NPGR010-2012%20-%2003-BRDF.pdf, 2012. [Accesed on 17. November 2013]

[15] Torrance, Kenneth E., Sparrow, E. *Theory for Off-Specular Reflection from Roughened Surfaces*. Optical Soc. America, vol. 57. 1976.

[16] Torrance, Kenneth E., Cook, Robert L. *A Reflectance Model For Computer Graphics*. Proc. SIGGRAPH, Computer Graphics, Volume 15, Number 3., August 1981, pp. 307-316.

[17] He, Xiao D., Torrance, Kenneth E., Sillion, Francois X., Greenberg, Donald P. *Comprehensive Physical Model for Light Reflection*. ACM SIGGRAPH, Computer Graphics, Volume 25, Number 4. July 1991.

[18] Germer, Thomas A.. *SCATMECH: Polarized Light Scattering C++ Class Library*. http://physics.nist.gov/Divisions/Div844/facilities/scatmech/, May 2008. [Accesed on 19. May 2013]

[19] Weidlich, A., Wilkie, A., Sillion, *Arbitrarily Layered Micro-Facet Surfaces*. In GRAPHITE 2007, pages 171–178, 2007.

[20] Elek, O. *Layered Materials in Real-Time Rendering*. CESCG2010, 2010.

[21] *Jones calculus*. Wikipedia, the free encyclopedia. http://en.wikipedia.org/wiki/Jones_calculus. [Accesed on 17. November 2013, 16:04].

[22] *SPIE*. Optipedia, Jones Calculus. http://spie.org/x32380.xml [Accesed on 17. 11. 2013, 16:17].

[23] *Basis (linear algebra)*. Wikipedia, the free encyclopedia. http://en.wikipedia.org/wiki/Basis_(linear_algebra). [Accesed on 29. November 2013, 13:30].

[24] *Rotation matrix*. Wikipedia, the free encyclopedia. http://en.wikipedia.org/wiki/Rotation_matrix. [Accesed on 29. November 2013, 15:45].

[25] *Rotation matrix*. Wikipedia, the free encyclopedia. http://en.wikipedia.org/wiki/Mueller_calculus. [Accesed on 2. December 2013, 7:00].

[26] *Total Internal Reflection*. Wikipedia, the free encyclopedia. http://en.wikipedia.org/wiki/Total_internal_reflection. [Accesed on 3. December 2013, 7:40].

[27] *Fresnel Equations*. Fresnel's Equations. http://hyperphysics.phy-astr.gsu.edu/hbase/phyopt/freseq.html. [Accesed on 3. December 2013, 7:30].

[28] *Total Internal Reflection*. Wikipedia, the free encyclopedia. http://en.wikipedia.org/wiki/Total_internal_reflection. [Accesed on 3. December 2013, 7:40].

Attachments

Attachment A

(* ki and kr are the incoming and outgoing unit propagation vectors *)

ki = {Sin [θ_i] , 0, −Cos [θ_i]} ;

kr = {Sin [θ_r] Cos [ϕ_r] , Sin [θ_r] Sin [ϕ_r] , Cos [θ_r]} ;

(* useful functions to normalize vectors and find perpendicular vectors *)

norm[v_]:=Sqrt[$v.v$]

unit[v_]:=v/norm[v]

perpto[v_, w_]:=unit[Cross[v, w]]

(*normal*)

zhat = {0, 0, 1}

(* the bases for defining polarisation in the scattering plane *)

nhat = unit[kr − ki];

sin = perpto[ki, nhat]//FullSimplify

srn = perpto[kr, nhat]//FullSimplify

pin = perpto[sin, ki]//FullSimplify

prn = perpto[srn, kr]//FullSimplify

(*thebasesfordefiningpolarisationinthe$s-p$bases*)

si = perpto[ki, zhat]//FullSimplify//PowerExpand

pi = perpto[si, ki]//FullSimplify//PowerExpand

sr = perpto[kr, zhat]//FullSimplify//PowerExpand

pr = perpto[sr, kr]//FullSimplify//PowerExpand

(*Thefollowingis$a$logicalresult,
howtocalculateasthereflectanceJonesmatrixinthe$s-$
$p$basis.Thematrixontherightfromthecentralmatrixconverts$a$vectorin(si, pi)basisto$a$vector
inthe(sin, pin)basis, whilethematrixontheleftconverts$a$vectorfromthe(srn, prn)basistothe
(sr, pr)basis.*)

$$\text{myReflectance} = \begin{pmatrix} \text{sr.srn} & \text{sr.prn} \\ \text{pr.srn} & \text{pr.prn} \end{pmatrix} . \begin{pmatrix} \text{Fs} & 0 \\ 0 & \text{Fp} \end{pmatrix} . \begin{pmatrix} \text{sin .si} & \text{sin .pi} \\ \text{pin.si} & \text{pin.pi} \end{pmatrix} \text{//FullSimplify}$$

(* The following in HTSG Eqs 4.14 *)

$$\text{JFsp} = \begin{pmatrix} \text{Fs(pi.kr)(pr.ki)} + \text{Fp(si.kr)(sr.ki)} & -(\text{Fs(si.kr)(pr.ki)} - \text{Fp(pi.kr)(sr.ki)}) \\ \text{Fs(pi.kr)(sr.ki)} - \text{Fp(si.kr)(pr.ki)} & \text{Fs(si.kr)(sr.ki)} + \text{Fp(pi.kr)(pr.ki)} \end{pmatrix} \text{//FullSimplify}$$

(*Theabovetwomatricesdon$'t$lookthesame.However,
thereis$a$suspectthattheyareproportionaltoeachotherandthatHTSGbroughtthesetermstogether
intosomeorallofthetermsinEq.4.15. Itcantestthiswiththefollowing...*)

myReflectance/JFsp/. {$\theta_i \to$ Random[], $\theta_r \to$ Random[], $\phi_r \to$ Random[], Fp → Random[], Fs → Random[]} //Simplify

(*Sincethesenumberalwayscomeoutthesame,
thatassertionwastrue.Itappearsweneedtodosome“reverse engineering”.We$'$regoingtoguessthat

```
someofthetermsinEq.4.15gointomakingthisratio1.00000andwefoundthatthecrossproduct
terminEq.4.15belongstotherotationmatrices.Wecanactuallyseethatitcomesfromthedefinitionsofthes−
vectorsbeingnormalized, asinEq.(42)intheoriginalHTSGarticle.*)
term1 = norm[kr − ki];
term2 = norm[Cross[kr, ki]];
term3 = zhat.(kr − ki);
myReflectance/(JFsp /term2^2)/. {θi → Random[], θr → Random[], ϕr → Random[], Fp → Random[], Fs → Random[]} //
Simplify

(*ThusmyReflectancematrixneedstobemultipliedbynorm[Cross[kr, ki]]^2inorderforittobeplug−
inreplaceableforEqs.4.14...*)
Jdd = ( Fs   0
        0   Fp ) norm[Cross[kr, ki]]^2//FullSimplify
```